EP Journal of Heat and Mass Transfer

Jan – April 2025 Vol – 9 Issue – 1

ENRICHED PUBLICATIONS

JE - 18,Gupta Colony, Khirki Extn,
Malviya Nagar, New Delhi - 110017.
E- Mail: info@enrichedpublication.com
Phone :- +91-8877340707

EP Journal of Heat and Mass Transfer

Aims and Scope

EP Journal of Heat and Mass Transfer is a peer reviewed journal published by Enriched Publication and articles are selected primarily on heat and mass transfer such as heat transfer in phase change phenomenon, machinery and welding operations turbulence etc. This journal consist of research articles and theoretical articles are also accepted of this subject.

EP Journal of Heat and Mass Transfer

EP Journal of Heat and Mass Transfer

(Volume - 9, Issue -1, 2025)

Content

Jan - April 2025 Vol – 9 Issue - 1

S. No.	Title	Authors	Pages
1.	Effect of Variation of High Temperature R1234ze Condenser Temperature and Intermediate R1234yf Temperature Cascade Condenser and Low Temperature Evaporator Circuit in three Stage Cascade Refrigeration Systems	R S Mishra	1-11
2.	Performance Analysis of Solar Air Conditioning: A Review	Ashok Kumar Yadav Vikram Pandey Sachin Singh Suyash Rai Abhinav Verma	12-18
3.	Thermoeconomic Comparative Analysis of Constructal and Conventional Heat Exchangers	Manjunath K.	19-37
4.	Heat Transfer in Microchannel Heat Sink: Review	Sunny Chandra Om Prakash	38-49
5.	Thermal Performance and Emission Test of CI Engine Using Biodiesel Produced from Waste Cooking Oil Blend With Diesel	Jatinder Kataria S.K. Mohapatra K. Kundu	50-65

Effect of Variation of High Temperature R1234ze Condenser Temperature and Intermediate R1234yf Temperature Cascade Condenser and Low Temperature Evaporator Circuit in three Stage Cascade Refrigeration Systems

R S Mishra

Department of Mechanical Preoduction & Industrial
and Automobiles Engineering, Delhi Technological University Delhi.
e-Mail: hod.mechanical.rsm@dtu.ac.in,

Abstract

The global warming and ozone depletion effects are well documented in the literature causes Climate change through global surface temperatures increase in the last century.For stoping this phenomenon, new regulations in terms of ban of CFC containing chlorine content refrigerants / greenhouse gas fluids (HFC among them) have been approved. Only low-GWP refrigerants will be allowed in developed countries. HFO fluids and most HFCs as refrigerants in HVACR systems possess similar thermo-physical properties such as that the most promising modern refrigerant is R1234ze and R1234yf. In this paper three stage cascade vapour compression refrigeration is proposed for industries (i.e. food, chemical, pharmaceutical and liquefaction of gases) using HFO-1234ze in the high temperature circuit and HFO-1234yf in intermediate temperature circuit and effect of eight ecofriendly refrigerants in the lower temperature circuit and best performance have been using R600 for better system's COP and second law efficiency with minimum exergy destruction ratio. And worst performances (i.e. lowest COP and higher exergy destruction ratio occurs using R407c .The numical computations have been carried out for three stages cascade refrigeration systems and optimum temperature range of components have been observed for optimum performances (i.e.minimum exergy destruction ratio alongwith optimum overall

(Maximum System coefficient of performance) occurs) at -45C of evaporator temperature and -5℃ of intermediate cascade evaporator optimum temperature.

Keywords- *Three stage VCR; Reduction in global warming; Ozone depletion; Energy-Exergy computation; first & second law analysis ; Ecofriendly refrigerants.*

Introduction

Low temperature cascade refrigeration systems using HFC134a, R507a , HCFC 22 HFC 123 and R508b in the high temperature circuit are normally required in the temperature range from -30 °C to -100℃ in the various industries such as food, chemical, pharmaceutical and liquefaction of gases such as nitrogen, helium hydrogen etc [1] . The application of multistage vapour compression refrigeration system is also not desirable for attaining very low temperatures due to the solidification temperature of the refrigerant and also low evaporator pressure with larger specific volume along with operational difficulties in the equipment with using single evaporator Gupta et.al [2] optimized the cascaded refrigeration-heat pump system using R-12 refrigerants in the higher temperature circuit and R-13 in low temperature circuit for optimum overall Coefficient of performance.

The exergy analysis of multistage cascade refrigeration system for natural gas liquefaction is carried out by Kanoğlu[3] in terms of performance parameters for exergy destruction and exergetic efficiency with minimum work requirement for liquefaction of natural gases.

Dopazo et al. [4] carried out the optimization of coefficient of performance of a cascade refrigeration system for cooling applications at low temperatures. in the variation of evaporation temperature range (- 55°C) to (-30°C) using CO2 in low temperature circuit, 25 to 50°C condensation temperature in high temperature circuit using NH3 and (-)25 to 5°C in cascade condenser. The overlapping (approach temperature) was varied between 3-6°C. The effect of compressor isentropic efficiency on system COP is also examined and also optained optimum condenser temperature.

The effect of HFOrefrigerants was not studied by them . Ratts and Brown [5] used the entropy generation minimization method an ideal cascade vapour compression cycle for determining the optimal intermediate temperatures. Bhattacharyya et al. [6] predicted the optimum performance of the cascade system with variation in the design parameters and operating variables by using CO2 in the high temperature cycle of about 120°C and C3H8 (Propane) in the low temperature cycle of about -40°C. Agnew and Ameli [7] used finite time thermodynamics approach for cascade refrigeration system refrigerants R717 in high temperature circuit and R508b low temperature circuit and found better performance in comparison to R12 in high temperature circuit and R13 low temperature. Nicola et al. [8] carried out first law performance analysis using ammonia in high temperature circuit of a cascade refrigeration system , blends of CO2 and HFCs in low temperature circuit of 216.58 K and observed that the ecofriendly CO2 (carbondioxide i.e. R744) blends are excellent options for the low-temperature circuit of cascade systems operating at temperatures arround 200 K. Lee et al. [9] carried out exergy analysis of a two stage cascade refrigeration system for ammonia and carbon dioxide for maximization of COP and minimization of energy loss by optimising condensing temperature and concluded that optimal condensing temperature increased with condensation and evaporation temperatures. Kruse and Rüssmann [10] computed COP of a cascade refrigeration system using NH3, C3H8, propene, CO2 for the high temperature stage of heat rejection temperatures between 25 to 55 °C and N_2O (Nitrous oxide) as refrigerant in the low temperature cascade stage and compared its result s with a conventional HFC134a cascade refrigeration system and observed that by replacing the lower stage refrigerant R23 by NO_2 have same energetic performance with high stage fluids R134a, ammonia and hydrocarbons. Niu and Zhang [11] compared experimental results of a cascade refrigeration system using R290 in high temperature circuit and a blend of R744/R290 in low temperature circuit with performance of with R13 in low temperature circuit and R290 in high temperature circuit and found that good cycle performance of blended R744/R290 in low temperature circuit gives promising performance by replacing R13 refrigerant by blends of R744/R290 when low temperature evaporator temperature is higher than 200 K. Getu and Bansal [10] studied the effect of evaporating, condensing and cascade condenser temperatures, sub-cooling and superheating in high temperature circuits and low temperature circuits and carried out energy analysis of a carbon dioxide–ammonia (R744/R717) cascade refrigeration system using multi-linear regression analysis and developed mathematical expressions for optimum COP using optimum evaporating temperature of R717 and the optimum mass flow ratio of R717 to that of R744 in the cascade system.

2. Performance Evaluatıon of three Stages Vapour Compressıon Refrıgeratıon System

The three stages cascade vapour compression refrigeration system choosen in this paper has is that tetrafluoropropene (HFO-1234ze) is a hydrofluoroolefin has zero ozone-depletion potential and a low global-warming potential (i.e. GWP = 6) was used in high temperature circuit which has as a "fourth generation" refrigerant to replaceR404a, R407c R-410a in the high temperature circuit in the range of -10C^o to 60$C^o$and in the intermediate temperature cycle HFO-1234yf is used because R1234yf is a new class of refrigerant acquiring a global warming potential (GWP) of (1/335th) that of R-134a (and around four times higher than carbon dioxide, which can also be used as a refrigerant in the intermediate temperature circuit between (-20^{o}C to -50^{o}C) which has properties significantly different from those of R134a, especially requiring operation at around five times higher pressure) and an atmospheric lifetime of about 400 times shorter. In the low temperature circuit R134a has zero ODP and 1300 GWP is very good Good performance in medium and low temperature applications because of very low toxicity and also not miscible with mineral oil and results were compared by using hydrogen carbon in the low temperature circuit has very promising non-halogenated organic compounds with no ODP and very small GWP values. Their efficiency is slightly better than other leading alternative refrigerants. Iso butane (R 600a) has : ODP-0,GWP-3 has higher boiling point hence lower evaporator pressure and also lowest discharge temperature alongwith very good compatibility with mineral oil. Similarly Propane (R290 has zero ODP- and -3 GWP is also compatible with copper miscible with mineral oil alongwith highest latent heat and largest vapour densityand third of original charge only is required when replacing halocarbons refrigerant in existing equipmentwith energy saving up to 20% due to lower molecular mass and vapour pressure. The Approximate auto ignition temperatures for R134a is 740 ºC, and For R600a is 470℃, and For R-290 is 465 °C respectively. The carbon dioxide has Zero ODP & GWP is also non flammable, non toxic, inexpensive and widely available and its high operating pressure provides potential for system size and weight reducing potential has draw back that operating pressure is very high side around 80 bars with low efficiency and only to be used up to -50 °C. The effect of Approach_1 (Overlapping temperature) means intermediate temperature circuit Condenser temperature –high temperature circuit Evaporator temperature and effect of Approach_2 (Overlapping temperature) means Low temperature circuit Condenser temperature –intermediate circuit Evaporator temperature on the performance are also highlighted in this paper.

3. Results And Dıscussıons

Following data have been considered for numerical computation

Condenser Temperature=50 [℃]

$Evaporator_{\_HTC}$=0.0 [℃]

$Evaporator_{\_ITC}$=-50.0 [℃]

$Evaporator_{\_LTC}$=-100.0 [℃]

Compressor $Efficiency_{\_HTC}$=0.80

Compressor $Efficiency_{\_ITC}$=0.80

Compressor $Efficiency_{\_LTC}$=0.80

$Approach_{\_ITC}$=10[℃]

$Approach_{\_LTC}$=10[℃]

As overlapping temperature is increasing the total exergy destruction ratio of the system is also increasing. Similarly by increasing low temperature circuit approach the second law efficiency , coefficient of performance of whole system is also decreasing along with decreasing low temperature as coefficient of performance shown in table-1(a) respectively. It was also observed that thre is no effect on COP of high temperature circuit using R1234ze (

COP=3.215) and also no effect on COP of intermediate temperature circuit using R1234yf (COP=2.204)and also similarly trends occurred by variation of approach (overlapping temperature between intermediate circuit condenser temperature and high temperature circuit evaporator temperature as shown in Table-1 (b) . As high temperature circuit condenser temperature increases along with total system exergy destruction ratio (EDR) the the overall COP and high temperature circuit COP are also is also decreases along with decreasing exergetic efficiency and no change of coefficient of performances of low temperature circuit (COP=2.204) and coefficient of performance of intermediate temperature circuit COP=1.79 as shown in Table-2. The table-3 shows the variation of evaporator temperature of high temperature circuit using HFO-1234ze from -20°C to +20°C. It was observed that exergetic efficiency and overall COP of system is increases and exergy destruction ratio decreases first and reached a range to a minimum level and then increases. The optimum performances of cascade systems occurs at intermediate cascade evaporator optimum temperature of -5°C.The variation of cascade evaporator of Intermediate circuit is increasing from -55C° to -30C,°The COP of LTC circuit is decreasing while The COP of ITC circuit is increasing along with increasing exergetic efficiency as shown in Table-4 respectively. It was also observed that there is a optimum (minimum) exergy destruction ratio alongwith optimum overall (Maximum System coefficient of performance) occurs at -45°C.Similarly the increasing temperature of LTC evaporator from -120°C to -90C° , the overall system COP and LTC COPis decreasing and exergy destruction ratio is increasing as shown in Table-5. The effect of various refrigerants used in low temperature circuit is shown in table-6 and it was observed that R600 gives better COP and better second law efficiency with minimum exergy destruction ratio while R407c gives lowest COP and higher exergy destruction ratio. It is seen that use of hydrocarbons are beneficial than using other ecofriendly refrigerants. R-134a is also used up to a temperature -100°C.

Table-1a: Effect of Overlapping temperature of low temperature condenser and Intermediate evaporator temperature Approach in the LTC of three stages Cascade Vapour compression Refrigeration systems using R1234ze in high temperature circuit and R1234yf in Intermediate temperature circuit and R134a in lower temperature circuit for a given data

Table-1b: Effect of Approach in the ITC of three stages Cascade Vapour compression Refrigeration systems using R1234ze in high temperature circuit and R1234yf in Intermediate temperature circuit and R134a in lower temperature circuit for a given data

Table-2: Effect of High temperature circuit condenser temperature in the LTC of three stages Cascade Vapour compression Refrigeration systems using R1234ze in high temperature circuit and R1234yf in Intermediate temperature circuit and R134a in lower temperature circuit for a given data

Approach_LTC	$COP_{Overall}$	COP_{LTC}	EDR_{System}	ETA_{Second}
0.0	0.570	2.247	1.428	0.4119
2.50	0.5535	2.116	1.50	0.3999
5.0	0.5376	1.998	1.574	0.3884
7.5	0.5222	1.889	1.650	0.3773
10.0	0.5074	1.790	1.728	0.3666

Table-1b: Effect of Approach in the ITC of three stages Cascade Vapour compression Refrigeration systems using R1234ze in high temperature circuit and R1234yf in Intermediate temperature circuit and R134a in lower temperature circuit for a given data

Approach_ITC	$COP_{Overall}$	COP_{ITC}	EDR_{System}	ETA_{Second}
0.0	0.5675	2.844	1.439	0.410
2.50	0.5522	2.663	1.587	0.3990
5.0	0.5371	2.97	1.577	0.388
7.5	0.5221	2.435	1.651	0.3773
10.0	0.5074	2.204	1.728	0.3666

Table-2: Effect of High temperature circuit condenser temperature in the LTC of three stages Cascade Vapour compression Refrigeration systems using R1234ze in high temperature circuit and R1234yf in Intermediate temperature circuit and R134a in lower temperature circuit for a given data

Condenser Temperature (^oC)	Overall System Performance $COP_{Overall}$	High temperature Circuit Performance COP_{HTC}	System Exergy Destruction Ratio EDR_{System}	Exergetic Efficiency ETA_{Second}
60	0.4530	2.47	2.055	0.3273
55	0.4804	2.779	1.881	0.3471
50	0.5074	3.215	1.728	0.3665
45	0.5340	3.737	1.592	0.3859
40	0.5606	4.379	1.469	0.4051
35	0.5873	5.192	1.356	0.4244
30	0.6143	6.264	1.253	0.4438
25	0.6416	7.750	1.157	0.4636

Table-3: Effect the HTC evaporator temperature of three stages Cascade Vapour compression Refrigeration systems using R1234ze in high temperature circuit and R1234yf in Intermediate temperature circuit and R134a in lower temperature circuit for a given data

High Temperature Circuit Evaporator Temperature (^oC)	Overall System Performance $COP_{Overall}$	High temperature Circuit Performance COP_{HTC}	System Exergy Destruction Ratio EDR_{System}	Exergetic Efficiency ETA_{Second}
20	0.4698	6.446	1.946	0.3395
15	0.4847	5.287	1.855	0.3502
10	0.4958	4.421	1.791	0.3583
5	0.5033	3.75	1.75	0.3637
0	0.5074	3.275	1.728	0.3666
-5	0.5081	2.78	1.724	0.3671
-10	0.5057	2.42	1.737	0.3654
-15	0.5003	2.117	1.766	0.3615
-20	0.4923	1.86	1.811	0.3557

Table-4: Effect the cascade intermediate evaporator temperature of three stages Cascade Vapour compression Refrigeration systems using R1234ze in high temperature circuit and R1234yf in Intermediate temperature circuit and R134a in lower temperature circuit for a given data

Cascade intermediate Circuit Evaporator Temperature (^oC)	Overall System Performance $COP_{Overall}$	High temperature Circuit Performance COP_{ITC}	Low temperature Circuit Performance COP_{LTC}	System Exergy Destruction Ratio EDR_{System}	Exergetic Efficiency ETA_{Second}
-30	0.5023	4.011	1.211	1.755	0.3629
-35	0.5067	3.404	1.328	1.731	0.3661
-40	0.5090	2.921	1.461	1.719	0.3678
-45	0.5092	2.529	1.613	1.718	0.3679
-50	0.5074	2.204	1.798	1.728	0.3666
-55	0.5035	1.931	1.998	1.749	0.3638

Table-5: Effect the Low temperature evaporator temperature(LTC) of three stages Cascade Vapour compression Refrigeration systems using R1234ze in high temperature circuit and R1234yf in Intermediate temperature circuit and R134a in lower temperature circuit for a given data

low Temperature Circuit Evaporator Temperature (^oC)	Overall System Performance $COP_{Overall}$	High temperature Circuit Performance COP_{LTC}	System Exergy Destruction Ratio EDR_{System}	Exergetic Efficiency ETA_{Second}
-90	0.5882	2.40	1.705	0.3697
-95	0.5470	2.067	1.712	0.3687
-100	0.5074	1.79	1.728	0.3666
-105	0.4693	1.556	1.753	0.3632
-110	0.4329	1.358	1.789	0.3586

Table-6: Effect the ecofriendly refrigerants temperature used in low temperature circuit evaporator of three stages Cascade Vapour compression Refrigeration systems using R1234ze in high temperature circuit and R1234yf in Intermediate temperature circuit for a given data

Ecofriendly Refrigerants	Overall System Performance $COP_{Overall}$	High temperature Circuit Performance COP_{HTC}	System Exergy Destruction Ratio EDR_{System}	Exergetic Efficiency ETA_{Second}
R123	0.5099	1.806	1.714	0.3685
R125	0.5020	5.287	1.757	0.3627
R404a	0.4971	4.421	1.784	0.3592
R134a	0.5074	3.75	1.728	0.3666
R407c	0.4367	3.275	2.169	0.3155
R290	0.510	1.807	1.714	0.3685
R600a	0.5123	1.822	1.701	0.3702
R600	0.5148	1.839	1.688	0.3720

Conclusions & Recommendations

The numical computations have been carried out in the three stages cascade refrigeration systems and following conclusions have been made.

1. There is a optimum (minimum) exergy destruction ratio alongwith optimum overall (Maximum System coefficient of performance) occurs at -45℃.
2. The optimum performances of cascade systems occurs at intermediate cascade evaporator optimum temperature of -5℃
3. R600 gives better COP and better second law efficiency with minimum exergy destruction ratio.
4. The minimum performances occurs

using R407c gives lowest COP and higher exergy destruction ratio

References

[1] Bansal, P. K. and Jain, Sanjeev(2007), Cascade systems: past, present, and future. ASHRAE Transactions; Vol-113,No.1: pp.245-252.

[2] Gupta V. K. (1985)Numerical optimization of multi-stage cascaded refrigeration-heat pump system. Heat Recovery Systems Vol.5, No.4: pp.305-319.

[3] Kanoğlu M. (2002)Exergy analysis of multistage cascade refrigeration cycle used for natural gas liquefaction. International Journal of Energy Research; Vol.26: pp.763–774.

[4] Dopazo J. A, Fernández-Seara J, Sieres J., Uhía F. J. (2009) Theoretical analysis of a CO2–NH3 cascade refrigeration system for cooling applications at low temperatures. Applied Thermal Engineering ,Vol- 29, No- 8-9, pp.1577-1583.

[5] Ratts E.B. and Brown J. S. (2000) A generalized analysis for cascading single fluid vapour compression refrigeration cycles using an entropy generation minimization method. International Journal of Refrigeration Vol.23:,pp.353-365.

[6] Bhattacharyya, S., Mukhopadhyay, S., Kumar A., Khurana R.K. and Sarkar J. (2005) Optimization of a CO2/C3H8 cascade system for refrigeration and heating. International Journal of Refrigeration; Vol.28,pp. 1284-1292.

[7] Agnew B. and Ameli S.M.(2004)A finite time analysis of a cascade refrigeration system using alternative refrigerants. Applied Thermal Engineering Vol-24: pp.2557–2565.

[8] Nicola G. D., Giuliani, G. , Polonara, F. and Stryjek, R.(2005) Blends of carbon dioxide and HFCs as working fluids for the low-temperature circuit in cascade refrigerating systems. International Journal of Refrigeration; Vol.28: pp.130–140. [

[9] Lee T. S., Liu C. H. and Chen T.W.(2006) Thermodynamic analysis of optimal condensing temperature of cascadecondenser in CO2/NH3 cascade refrigeration systems.

International Journal of Refrigeration;Vol.29:pp.1100-1108.

[10]Kruse, H. and Rüssmann, H. (2006)The natural fluid nitrous oxide-an option as substitute for low temperature synthetic refrigerants. International Journal of Refrigeration; Vol.29: pp.799-806.

[11] Niu, B. and Zhang, Y.(2007) Experimental study of the refrigeration cycle performance for the R744/R290 mixtures. International Journal of Refrigeration; Vol.30: 37-42.

[12]Getu, H.M., Bansal P.K. (2008); Thermodynamic analysis of an R744/R717 cascade refrigeration system. International Journal of Refrigeration, Vol.31, No.1:,pp.45- 54.

Performance Analysis of Solar Air Conditioning: A Review

Ashok Kumar Yadav
Associate Professor,Department of Mechanical Engineering,Raj Kumar Goel Institute of Technology, Ghaziabad, 201003, India, Email: ashokme015@gmail.com

Vikram Pandey, Sachin Singh, Suyash Rai, Abhinav Verma
B. Tech students,Department of Mechanical Engineering,Raj Kumar Goel Institute of Technology, Ghaziabad, 201003, India

Abstract

This paper represents a review of new solar based air conditioning techniques. These techniques used solar energy to produce cold or hot air and do not pollute the environment. Thermally driven cooling system is the key component of these systems. The use of solar powered air conditioning systems for heating and cooling requirements in the buildings would be more economical. Though various air conditioning systems run on solar power have been tested extensively, there have been very less focus on the use of solar powered air conditioning systems. Aim of this paper is to review the literature on emerging technologies for solar air conditioner and provide knowledge which will be helpful to initiate the study in order to investigate the influence of various parameters on the overall system performance

Keywords- solar air-conditioning; pcm; adsorption

Introduction

The demand for human comfort is increasing day by day. The International Institute of Refrigeration in Paris has estimated that approximately 15% of all the electricity produced in the whole world is employed for refrigeration and air-conditioning processes of various kinds, and the energy consumption for air-conditioning systems has recently been estimated to be 45% of the whole households and commercial buildings. Most of this demand is being met by vapour compression based refrigeration system. Recently, though nominal, some vapour absorption based refrigeration systems have come for industrial and office building use. Solar energy can be used for air-conditioning in two ways – electricity through solar photo-voltaic cell and then using the same in conventional i.e. vapour compression cycle and the heat driven sorption system. The improvement in solar photo-voltaic cell efficiency is very slow and so initial cost is very high till now. Among the heat driven systems, vapour absorption systems are already commercially available, but mostly having capacity of more than 30 TR. They have limitations for smaller capacity.

2. Main Components In Solar Air-Conditioning

The main components in the solar assisted air conditioning system can be divided into five main components namely:-

1. Solar collector
2. Hot water & chilled water storage
3. Chiller (cold production)
4. Cooling towers
5. Fan coils

3. Solar Air Conditioners

Grenier et al. [1] built a large cold store of volume 12 m3 powered by solar energy using a zeolite 13-water combination.The evaporator temperature achieved was as low as 2.5 8C, corresponding to a solar COP of 0.086. Comparing these results reveals that the technology does not show any size advantages and, therefore, could be adaptable to large, small and medium size refrigerators. Sakoda and Suzuki [2] constructed and tested a laboratory scale closed adsorption cooling system employing a silica gel–water combination. The successful operation of this unit demonstrated clearly both the experimental and technical feasibility of solid adsorption refrigeration.

4. Solar Ice Makers

Critoph [3] built a laboratory scale activated carbon–ammonia refrigerator. The evaporator temperature attained was up to _1 8C and about 3 kg of ice was manufactured. The peak collector temperature for the simulated day tests was 115 8C, and the solar COP was 0.04. Although the COP and ice production of this machine are less than those of an activated carbon–methanol pair machine, activated carbon–ammonia system is less sensitive to small leakages, which makes it more reliable for application in remote areas where maintenance is not readily available.

Wang et al. [4] proposed a solar-powered continuous solid adsorption refrigeration and heating hybrid system. A solar water heater and an adsorption icemaker are joined in the same machine.The machine used the working pair activated carbon–methanol and had 2 m2 of evacuated tube collectors to warm 60 kg of water up to 90 8C. The daily ice production was about 10 kg when the insolation was about 22 MJ/m2.

5. **The Process**

Rastogi et al. [5] discussed about commercialization of Phase Change Materials (PCMs) for heating, ventilation and air-conditioning (HVAC) applications, has paved way for effective utilization of ambient thermal fluctuations. They attempted to extend Multiple Criteria Decision Making (MCDM) approach for ranking and selecting PCMs for domestic HVAC application. The graded materials were ranked using Technique for Order Preference by Similarity to Ideal Solution (TOPSIS). It was observed that the results obtained by simulation are in good agreement with those obtained using MCDM approach. The candidates with the best ranks showed significant improvement in ameliorating the temperature conditions. Thus it can be concluded that integration of MCDM approach for PCMs selection would prove to an economical and swift alternative technique for ranking and screening of materials. Through the proposed work, the authors have attempted to screen and rank various commercial Phase Change Materials for heating, ventilation and air-conditioning application. A Multiple Criteria Decision Making approach was used for this purpose. Suitable materials were first shortlisted based on the phase change temperature (within the range of 17–25^{0}C).

Prasartkaew et al [6] Renewable energy based technologies can be introduced for building cooling applications. Most studies on solar absorption cooling use fossil energy based auxiliary heaters. The results demonstrate that the system operates at about 75% of nominal capacity at an average overall system coefficient of performance of about 0.11. Performances of individual components of the system were also evaluated. The experimental results compared with results from other studies shows that the proposed system's performance in terms of chiller and overall system coefficient of performance is superior. The results demonstrate that the system operated at about 75% of nominal capacity and an average overall system coefficient of performance of about 0.11 was achieved. The results also show that, due to the limitation of heat absorption at the evaporator of this (small size) chiller, the supplied excess heat was rejected at the cooling tower. The biomass-gasifier boiler system, used as a booster/auxiliary heater, can improve the overall system performance. Comparison of performance of solar cooling system with different auxiliary heat sources shows that the proposed system outperforms the others, in terms of chiller and overall system coefficient of performance.

Bach et al. [7] used is a solid adsorption system to describe a new solar based air conditioning techniques. Suggested design procedure is simple and does not require a high technology. This type of unit can be used widely in the regions with an abandoned solar resource.

Younes et al.[8] studied Lithium – Bromide absorption machine thoroughly, showing the amount of fuel used in last few years for air conditioning. Also by studying each main part of the machine and different parameter; it was found that the length of the tubes required can be calculated to ensure the transfer of heat. This study showed that the machine needs six years and eight months to retain its costs with an annual payback of $120000.

Xia et al. [9] applied for a patent of a silica gel–water adsorption chiller driven by a low temperature heat source that was used to cool a grain depot in the Jiangsu Province, China. This chiller has two identical chambers and a second stage evaporator with methanol as working fluid. Each chamber contains one adsorber, one condenser and one evaporator (the first stage evaporator).

Li et al. [10]. The estimated thermal COP is about 0.4 under the following operating conditions: condensing temperature 40 8C, evaporating temperature 10 8C, regenerating temperature 120 8C and desorbing temperature 200 8C, using zeolite 13_–water as the working pair.

Yadav et al. [11] discussed about Peltier effect with which one can cool a specific area without using compressor which take a huge consumption of electricity.This system is driven by solar energy using solar plates, battery, transformer peltier module and heat sink. The analysis showed that for the prevalent conditions the compressor less AC is significantly more economical to own and operate than the conventional AC. In spite of a slightly higher initial cost, the thermoelectric AC proves to be more economical, mainly due to its significantly lower operating cost.

Wang [12] compared the COP of adsorptions systems with and without mass recovery and found that the former could produce a COP from 10% to 100% higher than the latter. The differencebetween the COPs was higher at lower generation temperatures.

in brief above work is reported in below table1

Author	Work study	Result
Rastogi et al.[5]	Phase change material (Pcm's)	MCDM proved to be a suitable technique to choose suitable pcm
Prasartkaew et al. [6]	COP of renewable energy in cooling applications	Superior results in terms of solar chillers
Wang et al. [4]	Solar adsorption and heating hybrid system	daily ice production was about 10 kg when the insolation was about 22 MJ/m^2
Critoph. [3]	Activated carbon ammonia refrigerator	advantages and limitations of the simultaneous transport of heat and adsorbate in a closed type adsorption cooling system.

6. Major Issues

The adsorption systems must have their size and cost reduced to become more commercially attractive. The most promising alternatives to achieve these goals include the enhancement of the internal and external heat transfer of the adsorber to increase the SCP, and the improvement of the heat management to increase the COP. The main technologies to enhance the external heat transfer in the adsorber are related to the increase of the heat exchange area, the use of coated adsorbers and the utilization of heat pipe technology. To improve the internal heat transfer, the most suitable option is the employment of consolidated adsorbents.

Conclusions

The principal challenge for adsorption refrigerators powered by solar energy is to overcome several failed attempts to commercialize them. Although investment costs for adsorption chillers using silica gel are still high, the environmental benefits are impressive , when compared to conventional compressor chillers. The absence of harmful or hazardous products such as CFCs, together with a substantial reduction of CO2 emissions due to very low consumption of electricity, creates an environmentally safe technology. Low temperature waste heat or solar energy can be converted into a chilling capacity as low as 5 8C with minor maintenance costs. Finally solar air conditioning has proved to be a good alternative for vapour compression system.

Refresnces

[1] Grenier Ph, Guilleminot JJ, Mester M, Meunier F, Pons M. Experimental results on a 12 m3 solar powered cold store using the intermittent zeolite 13–water cycle. In: Szokolay SV, editor. Solar World Congress, vol. 1 (1). Pergamon Press; 1984. p. 353.

[2] Sakoda A, Suzuki M. Simultaneous transport of heat and adsorbate in closed type adsorption cooling system using solar heat. J Sol Eng 1986;108:239.

[3] Critoph RE. Laboratory testing of an ammonia carbon solar refrigerator. In: ISES, Solar World Congress; 1993.

[4] Wang RZ, Li M, Xu YX, Wu JY. An energy efficient hybrid system of solar powered water heater and adsorption ice maker. Sol Energy 2000;68:189–95.

[5] Monisha Rastogi, Aditya Chauhan, Rahul Vaish , Anil Kishan, Selection and performance assessment of Phase Change Materials for heating, ventilation and air-conditioning applications, 2014.

[6] Boonrit Prasartkaew, S. Kumar , Experimental study on the performance of a solar-biomass hybrid air-conditioning system, 2003.

[7] Habib Ben Bacha, MounirElleuch, MounirBaccar, Aref Y. Maalej, Hamed Ben Dhia Air Conditioning By Solar Energy" Journal of Electron Devices,Vol. 2, pp. 40-44, 2003.

[8] R. Younès, H. Zeidan, H. Harb, *A. Ghaddar* Optimal Design And Economical Study For Solar Air-Conditioning By Absorption Chillers‖ International IIR conference on latest developments in refrigerated storage, transportation and display of food products Amman- Jordan, 28-30 March 2005.

[9] Xia ZZ, Wang RZ, Wu JY, Wang DC. New type of effective adsorption chiller adopting separate heat pipe. China Patent 200410025398.0, 2004.

[10] Li CH, Wang RZ, Lu YZ. Investigation of a novel combined cycle of solar powered adsorption–ejection refrigeration system. Renew Energy 2002;26:611–22.

[11] Yadav, A. K., Singh, S., Gupta, G., Solar Air-Conditioning: Design for a Compressor-Less System using Peltier Effect, International Journal of Advance Research and Innovation, 2014 , vol. 2, no.2, pp. 429-432

[12] Wang RZ. Performance improvement of adsorption cooling by heat and mass recovery operation. Int J Refrig 2001;24:602–11.

Thermoeconomic Comparative Analysis of Constructal and Conventional Heat Exchangers

Manjunath K.
Department of Mechanical Engineering, Delhi Technological University, Bawana Road, Delhi.
e-mail manjukmys@gmail.com

Abstract

Second law entropy generation and thermoeconomic analysis is carried out to find out the performance of constructal heat exchanger compared to conventional or normal heat exchanger. In the constructal heat exchanger, flow of the fluid stream is considered from the trunk to the branches that is the diameter and the length of the constructs keep on reducing at each subsequent bifurcation level. Second law of thermodynamic analysis is used as performance parameter to compare the constructal and the normal heat exchangers on the basis of entropy generation numbers, NTU, effectiveness and thermoeconomic cost. From the results, it can be concluded that constructal heat exchanger is having higher performance compared to normal heat exchanger. This is because of the contructal law based dendritic design of heat exchanger is having lower resistance to fluid flow and having global constraint of minimum volume structure.

Keywords- *Constructal law; tree-shaped heat exchangers; entropy generation minimization; thermoeconomic; heat transfer irreversibility; pressure drop irreversibility.*

Introduction

Heat exchangers are one of important components used in almost all the equipments or systems. Its design and operation in optimize manner is at most requirement to achieve energy conservation and to reduce global warming. The heat exchange research is in the direction to achieve better performance by finding new ways of thermal design, construction and operation. For this objective, the best choice is to adopt constructal law and entropy generation minimization methods for heat exchanger analysis. By constructal theory we can also identify the geometric configuration that maximizes performance subject to several global constraints [1]. Maximum thermodynamic performance is achieved by minimization of the entropy generated in the assemblies. Tree networks represent a new trend in the optimization and miniaturization of heat transfer devices. Constructal theory is used to optimize the performance of thermo-fluid flow systems by generating geometry and flow structure, and to explain natural self-organization and self-optimization. Bejan [1] stated the constructal law as “For a finite-size system to persist in time (to live), it must evolve in such a way that it provides easier access to the imposed (global) currents that flow through it”. The optimal structure is constructed by optimizing volume shape at every length scale, in a hierarchical sequence that begins with the smallest building block, and proceeds towards larger building blocks (which are called 'constructs') [2-5].

Bejan [6] described the constructal route to the conceptual design of a two-stream heat exchanger with maximal heat transfer rate per unit volume and gave the advantages of the tree-like (vascularized) heat exchanger structure over the use of parallel small-scale channels with fully developed laminar flow. Chen and Cheng [7] proposed a fractal tree-like micro-channel net heat sink for the cooling of electronic chips. The micro-channel net was designed to have a top and a bottom circulation pattern in a wafer. The study showed that this type of heat sink had better heat transfer characteristics and required less pumping power than traditional parallel nets. Zamfirescu and Bejan [8] investigated constructal tree-shaped two-phase flow for cooling a surface. They studied the optimal structure of the phase change with convective heat transfer. Bonjour et al. [9] investigated the heat exchange process with counter flows in two coaxial pipes, and optimized the fin set between the two pipe walls.

Da Silva et al. [10] described the conceptual design and performance of balanced two-stream counter flow heat exchangers, in which each stream flows as a tree network through its allotted space. The two trees in counter flow are like two palms pressed against each other. They developed the relationships between effectiveness and the number of heat transfer units for several tree-counter flow configurations. Muzychka [11] studied constructal design of force convection cooled microchannel heat sinks and heat exchangers. They investigated the heat transfer performances of different shapes of micro-channels involving parallel plates, rectangles, squares, ellipses, rounds, triangles and polygons. Raja et al. [12] studied the constructal optimization problem of heat exchangers by using air and water as the heat exchange mediums, and performed numerical calculations for the fluid flow and heat transfer problems.

Zimparov et al. [13] used the concepts of da Silva et al.[10] to analyze the performance of balanced two-stream parallel flow constructal heat exchangers. Zimparov et al. [14, 15] optimized the performance of several classes of simple flow systems consisting of T- and Y-shaped assemblies of ducts, channels and streams. Maximum thermodynamic performance was achieved by minimization of the entropy generated in the assemblies. Raja et al. [16] proposed the design and analysis of a multi-block heat exchanger by applying the concept of constructal theory. The experimental result confirms the effectiveness enhancement when compared to that of the conventional heat exchanger.

The hydrodynamic performance of the network, composed of a series of rough ducts, for both laminar and turbulent flow regimes was studied by Miguel [17]. Transient response of internal fluid pressure is also modelled and analyzed. Kim et al. [18] showed numerically how the geometric configuration of the tubular flow structure controls the global performance of a cross-flow heat exchanger. Constructal analysis of tree-shaped microchannels for flow boiling in a disc-shaped body has been carried out to achieve an energy efficient design for chip cooling by Daguenet-Frick et al. [19]. They tried to determine the best architecture that minimizes the thermal resistance for a given pressure drop under several constraints.

Flow boiling in a constructal tree-shaped minichannel network was numerically investigated using a one-dimensional model, taking into consideration the minor losses at junctions by Zhang et al. [20]. The new approach of constructal theory has been employed to design shell and tube heat exchangers by Azad and Amidpour [21]. The results of design using constructal theory are heat exchangers with in-series sections which are called constructal shell and tube heat exchangers. Kim et al. [22] developed analytically the constructal design of steam generators with a large number of tubes. The main features of a steam generator are determined based on the method of constructal design. Hajmohammadi et al. [23] studied the dual effect of size and spacing of a finite number of heat sources theoretically solving the governing equations numerically. Constructal theory was systematically applied to determine the optimal configuration of heat sources in the array. The results showed that when the freedom to morph is increased, more global objectives are smoothly achieved. Heat exchanger optimization procedure based on entropy generation and second law analysis have been reviewed by Awad and Muzychka [24].

Lee et al. [25] analyzed systematically the effect that the freedom to morph the flow configurations has on the performance of the comb-like tree network for the vascularization of smart materials with self-healing and self-cooling functionalities. The search for better flow architectures is achieved by endowing the flow network with more degrees of freedom to morph the flow configuration: diameter and aspect ratios and system sizes. Lorente et al. [26] explored the opportunity to maximize the production of power in a steam-turbine power plant by properly configuring the hardware at the interface between the stream of hot gas produced by the furnace and the steam that circulates through the power producing cycle. The interface consists of four heat exchangers, superheaters and reheaters, in parallel flow and counter flow.

Manjunath [27] used entropy generation minimization method to analyze different configurations of constructal heat exchangers designed by Bejan. Comparison of several tree-heat exchanger configurations such as: trees covering uniformly a rectangular area, trees on a disk shaped area, and trees on a square-shaped area are studied based on heat transfer and pressure drop entropy generation formulations by varying number of pairing levels and initial length-to-diameter ratio for best performance. Hajmohammadi et al. [28] proposed a new technique to enhance the heat transfer from a discretely heated pipe to a developing laminar fluid flow. Applying this technique, the effective length of the thermal entrance region is enlarged and as a result, the average heat transfer is invigorated. In order to maximize the heating performance, an optimal placement of the insulated segments between the heated segments is calculated according to constructal design. Hajmohammadi et al. [29] explored the bearing that a non-uniform distribution of heat flux used as a wall boundary condition exerts on the heat transfer improvement in a round pipe. The main conclusion that was drawn from their work is the emergence of a novel technique to enhance the heat transfer from a heated pipe under conditions of both fully-developed and developing laminar fluid.

Bejan et al [30] determined the fundamental relation between global performance and flow configuration (constructal design) in the case of steam power generation with superheater and reheater placed in parallel in the same stream of hot gases of combustion. Errera et al. [31] analyzed the relationship between complex flow architecture and global performance for assemblies of heat pumps coupled thermally with the ground through a single U-shaped loop with circulating fluid. The relationship between flow architecture and global performance (heat transfer density) serves as guide for the energy design of high-density urban settlements in the future.

Based on constructal theory, entropy generation minimization and second law efficiency equations are formulated for tree-shaped counter flow imbalanced heat exchanger for fully developed laminar and turbulent fluid flow by Manjunath and Kaushik [32]. Entropy generation number, rational efficiency and effectiveness behaviour with respect to changes in number of pairing levels and different tube length-to-diameter ratios of constructal heat exchanger are analyzed analytically. Comparison of a constructal heat exchanger and normal heat exchanger is analyzed by using second law analysis by Manjunath and Kaushik [33]. Analysis is carried out by considering the three irreversibilities due to heat transfer, pressure drop and production of the materials and the construction of the heat exchanger. Manjunath and Kaushik [34] reviewed heat exchanger analysis based on second law thermodynamics and constructal law. They also provided the basic thermal design procedure of different heat exchangers based on second law and constructal theory in-depth.

In this analysis, the importance of constructal theory in the thermal design of heat exchangers is studied and discussed. For this purpose we need to perform comparison between constructal heat exchanger (CHE) versus normal heat exchanger (NHE) which is the existing as single dimensioned tubes in conventional form. To compare these heat exchangers thermodynamically we need a technique which incorporates all important performance parameters in a single closed form equation. Second law of thermodynamic offers this technique which incorporates all the losses in terms of entropy generation rate or irreversibilities in a single formulation. The performance parameter which is popular in second law of thermodynamics is Bejan's entropy generation number. This is being a non dimensional number is a perfect parameter for the analysis of thermal systems like heat exchangers which is able to provide real behavior along with first law analysis. Two cases of comparison is carried out, one considering same heat exchanger surface area between CHE and NHE, another considering same heat exchanger tube volume. The analysis is carried out by the variation of entropy generation minimization numbers due to heat transfer and pressure drop. The behavior of entropy generation number and effectiveness is analyzed by varying number of constructal pairing level.

2. Analysis

The assumptions made while carrying out the analysis are: 1. The flow is fully developed, 2. Every tube is slender, and the flow is in the Poiseuille regime, the pressure drops are mainly due to friction along the straight cross section of the heat exchanger, 3. Neglecting the local pressure drops associated in the joints of the tubes, 4. One tube of hot stream tree is right next to its counterpart in the cold stream tree and has excellent thermal contact, 5. The same type of fluid is flowing in both the streams. 6. The heat exchanger is a balanced one.

Here in our analysis, the sizes of tubes of the constructal heat exchangers decrease from higher dimensions to lower. Each tree is made up of tubes of (n+1) sizes. Each tube has the length L_i and internal diameter D_i, where i = 0,1, . . . ,n. Tube lengths halves after two consecutive construction steps. For the entire tree structure the length-halving formula can be expressed approximately [2]

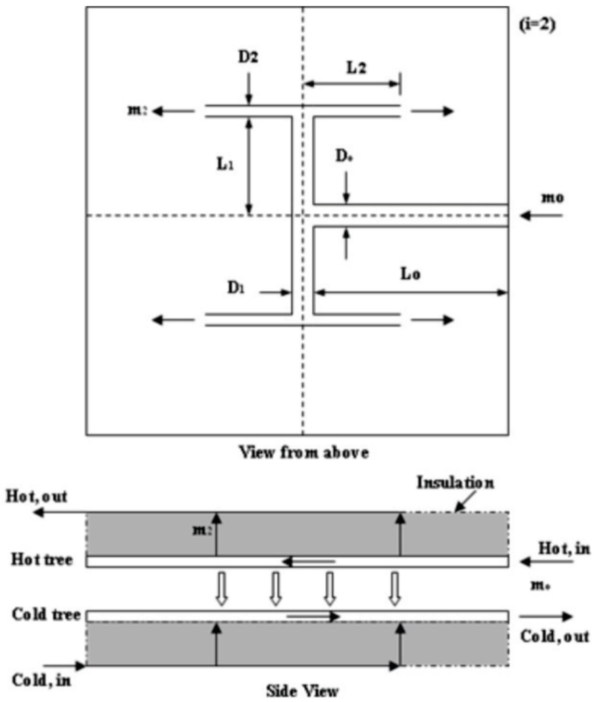

Figure 1. Counter flow of tree shaped streams distributed over a square area [10]

(1)

As we considered pairing at every construction level, the tube numbers and flow rates are expressed as,

$$n_i = 2^{-n-i} \qquad (2)$$

and $$\dot{m}_i = 2^{-i}\,\dot{m}_o \qquad (3)$$

For n level of construction stages, at the end, the stream mass flow rate will be m_n that is equal to flows through the nth construct. The inner diameter of the tube is decremented as given by [2],
The stream-to-stream heat transfer

$$\frac{D_{i+1}}{D_i} = 2^{-1/3} \qquad (4)$$

rate of the exchanger is given as,
Assuming that the heat transfer rate is

$$Q_i = U_i \pi D_i L_i \Delta T_i \qquad (5)$$

impeded primarily by the internal (convective) thermal resistances of the two flows and not by the thermal diffusion through the material in which the tube pair is embedded [10]. Considering the same type of fluid flowing in both the tubes, the overall heat transfer coefficient is given as,

$$\frac{1}{U_i} = \frac{1}{h_i} + \frac{1}{h_i}$$

The heat transfer coefficient is related to the Nusselt number as,

$$h_i = \frac{k}{D_i} Nu \tag{6}$$

The NTU expression provided by da Silva et al. [10] considering stream-to-stream heat transfer and enthalpy difference heat transfer is given as,

$$NTU_i = \frac{\pi k Nu L_i}{2 \dot{m}_i c_p} \tag{7}$$

The entropy generated in the heat exchanger by considering irreversibilities due to heat transfer and pressure drop is given by Bejan [35] as,

$$\dot{S}_{gen,i} = \left(\dot{m}c_p\right)_c \ln\left(\frac{T_{c,out}}{T_{c,in}}\right) + \left(\dot{m}c_p\right)_h \ln\left(\frac{T_{h,out}}{T_{h,in}}\right) - \left(\dot{m}R\right)_c \ln\left(\frac{p_{c,out}}{p_{c,in}}\right) - \left(\dot{m}R\right)_h \ln\left(\frac{p_{h,out}}{p_{h,in}}\right) \tag{8}$$

Defining the entropy generation number by dividing entropy generation by minimum heat capacity rate [35],

$$N_{s,i} = \frac{\dot{S}_{gen,i}}{\left(\dot{m}_i c_p\right)_{\min}} \tag{9}$$

If we consider a balanced heat exchanger, the entropy generation numbers due to heat transfer and pressure drop takes the form respectively as,

$$N_{sh,i} = \frac{\tau^2}{NTU_i} \tag{10}$$

$$N_{sp,i} = 2\left(\frac{R}{c_p}\right)\left(\frac{G_i^2 f}{2\rho P_r St}\right) NTU_i \tag{11}$$

Where P is the reference pressure which is taken equal to the inlet pressure of the cold stream and the constant τ^2 is defined as,

$$\tau^2 = \frac{\left(T_{h,in} - T_{c,in}\right)^2}{T_{c,in} T_{h,in}} \tag{12}$$

In the analysis, it is assumed for simplicity that the value of τ is same for the whole heat exchanger and it corresponds to the very first entry of hot and cold fluids streams temperatures. This assumption holds good because, in our analysis we have considered balanced heat exchanger and the temperature difference between the streams, ΔT remains constant throughout as specified in [10].

The total entropy generation number is the sum total of all the entropy generation numbers,

$$N_{s,i} = N_{sh,i} + N_{sp,i} \quad (13)$$

Case 1: For same volume between CHE and NHE

Volume of the NHE is given as,

$$V_o = \frac{\pi}{4} D_o^2 L \quad (14)$$

The total duct volume of CHE is given as,

$$V_n = \frac{\pi}{4} D_o^2 L_o S_1 \quad (15)$$

Where

$$S_1 = \frac{1 - \left[2.2^{(-1/3)^2} 2^{(-1/2)}\right]^{n+1}}{1 - 2.2^{(-1/3)^2} 2^{(-1/2)}} \quad (16)$$

The value of the tube length of the NHE for the specified value of number of pairing levels, n of the CHE can be obtained by equating equations (14) and (15) for same volume case as,

$$L = L_o S_1 \quad (17)$$

Case 2: For same surface area between CHE and NHE

Surface areas of the heat exchanger tube of CHE and NHE are respectively given as,

$$A_{s,n} = \pi D_o L_o S_2 \quad (18)$$

Where

$$S_2 = \frac{1 - \left[2.2^{(-1/3)} 2^{(-1/2)}\right]^{n+1}}{1 - 2.2^{(-1/3)} 2^{(-1/2)}} \quad (19)$$

$$A_{s,o} = \pi D_o L \quad (20)$$

Now, the value of the tube length of the NHE for the specified value of number of pairing levels, n of the CHE can be obtained by equating equations (18) and (20) for same surface area case as,

$$L = L_o S_2 \quad (21)$$

For the CHE, the stream-to-stream heat transfer rate is obtained by the summation of the local expression of equation (5) for the whole configuration as [10],

$$\dot{Q}_n = \sum_{i=0}^{n} \dot{Q}_i \quad (22)$$

$$\dot{Q}_n = 2^{-1} \pi k Nu \Delta T . L_o S_3 \quad (23)$$

Where

$$S_3 = \frac{1 - \left[2^{(-1/2)}\right]^{n+1}}{1 - 2^{(-1/2)}} \quad (24)$$

Where ΔT is the stream-to-stream

temperature difference which remains the same throughout the balanced heat exchanger.
For the NHE, the stream-to-stream heat transfer rate is given as,

$$Q_o = 2^{-1} \pi k Nu \Delta T.L \quad (25)$$

Considering a suitable value for the Reynolds number, we are able to calculate the mass flow rate of fluid in NHE as,

$$\dot{m}_o = \frac{\mu \operatorname{Re} A_{c,o}}{D_o} \quad (26)$$

Where $A_{c,o}$ is the cross sectional area based on the inside diameter of the NHE tube. Likewise, the mass flow rate of fluid in CHE is calculated as,

$$\dot{m}_n = \frac{\pi \mu \operatorname{Re} D_o S_4}{4} \quad (27)$$

Where

$$S_4 = \frac{1 - \left[2.2^{(-1/3)}\right]^{n+1}}{1 - 2.2^{(-1/3)}} \quad (28)$$

For the CHE, the NTU expression is obtained by the summation of the local expression of equation (7) for the whole configuration as provided in [10],

$$NTU_n = \sum_{i=0}^{n} NTU_i \quad (29)$$

$$NTU_n = \frac{\pi k Nu L_o S_3}{2 \dot{m}_n c_p} \quad (30)$$

For NHE, the NTU expression is given as,

$$NTU_o = \frac{\pi k Nu L}{2 \dot{m}_o c_p} \quad (31)$$

The effectiveness relationship for the balanced counter flow of the CHE and NHE are respectively given as,

$$\varepsilon_n = \frac{NTU_n}{NTU_n + 1} \quad (32)$$

$$\varepsilon_o = \frac{NTU_o}{NTU_o + 1} \quad (33)$$

The heat transfer entropy generation number for the CHE is obtained by the summation of the local expression of equation (10) for the whole configuration as,

$$N_{sh,n} = \sum_{i=0}^{n} N_{sh,i} \quad (34)$$

$$N_{sh,n} = \frac{\tau^2}{NTU_n} \quad (35)$$

The heat transfer entropy generation number for the NHE is given as,

$$N_{sh,o} = \frac{\tau^2}{NTU_o} \quad (36)$$

The mass velocity for the CHE is obtained as,

$$G_n = \frac{m_n}{A_{c,n}} = \frac{m_n}{(\pi/4)D_o^2 S_5} \quad (37)$$

Where

$$S_5 = \frac{1-\left[2.2^{(-1/3)^2}\right]^{n+1}}{1-2.2^{(-1/3)^2}} \quad (38)$$

Where $A_{c,n}$ is the cross sectional area based on the inside diameter of the CHE tube. The mass velocity for the NHE is obtained as,

The pressure drop entropy generation

$$G_o = \frac{m_o}{A_{c,o}} = \frac{m_o}{(\pi/4)D_o^2} \quad (39)$$

number for the CHE is obtained by the summation of the local expression of equation (11) for the whole configuration as,

The pressure entropy generation

$$N_{sp,n} = \sum_{i=0}^{n} N_{sp,i} \quad (40)$$

$$N_{sp,n} = 2\left(\frac{R}{c_p}\right)\left(\frac{G_n^{\ 2} f}{2\rho P_r St}\right) NTU_n \quad (41)$$

number for the NHE is obtained as,

The thermo economic cost (total cost)

$$N_{sp,o} = 2\left(\frac{R}{c_p}\right)\left(\frac{G_o^{\ 2} f}{2\rho P_r St}\right) NTU_o \quad (42)$$

of the heat exchanger is given as the sum of the capital cost and the irreversibility penalty costs as

$$C_i = C_{e,i}.R_c.\phi + C_s.H.\dot{I}_{t,i} \quad (43)$$

provided in [34],

Where $C_{e,i}$ is the cost of the equipment which is considered to be proportional to the surface area of the heat exchanger which includes the material and production cost. Production cost of the heat exchanger includes the secondary manufacturing processes like tube bending, welding, assembling, etc. The cost of insulation is ignored. While Φ is the operation maintenance factor, C_s is cost associated with the irreversibilities which is taken as equal to the electricity cost and H is the number of operation hours in a year.

R_c is the capital recovery factor given as,

$$R_c = \frac{i_e(1+i_e)^{l_c}}{(1+i_e)^{l_c}-1} \quad (44)$$

Where i_e the effective rate of return, l_c is is the technical life or life cycle in years.

The thermoeconomic cost (total cost) expressions for the CHE and NHE is obtained from procedures provided from Equations (43) to (44) respectively as,

$$C_n = C_{e,n}.R_c.\phi + C_s.H.\dot{I}_{t,n} \quad (45)$$

$$C_o = C_{e,o}.R_c.\phi + C_s.H.\dot{I}_{t,o} \quad (46)$$

Where the irreversibilities is expressed in terms of the product of the entropy generation rate and reference temperature T_r is given as,

$$\dot{I}_t = T_r\, \dot{m}_o\, c_p N_s \quad (47)$$

3. Results and Discussion

Input values considered for the analysis are: initial tube inside diameter (D_o = 0.005 m), length-to-diameter ratio (L_o/D_o = 120) as specified in [37], temperature ratio (T_{hi}/T_{ci} = 1.5), inlet cold temperature (T_{ci} = 300 K), inlet cold pressure (P_{ci} = 10^5Pa), pressure ratio (P_{hi}/P_{ci} = 8), reference temperature (T_r = T_{ci}), reference pressure (P_r = P_{ci}), Reynolds number (Re = 1500) for a fully developed laminar flow and (Re = 10^5) for a fully developed turbulent flow, The two stream fluids in the heat exchanger are considered as air and its thermo physical properties are referenced at average temperature from [39]. The results are obtained by using Engineering equation solver [40] software. Comparison of CHE and NHE by the variation of number of constructal level is carried out.

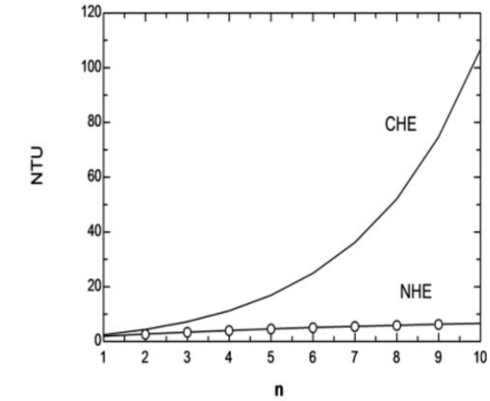

Figure 2. NTU versus number of pairing levels for the case of same volume.

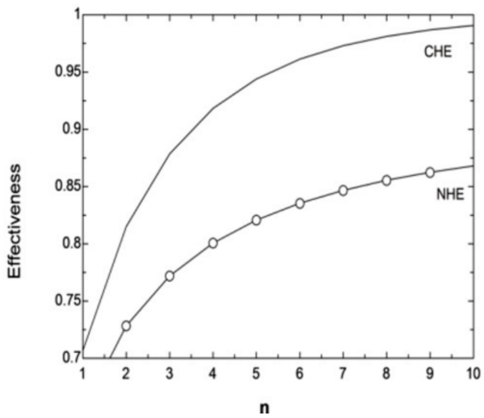

Figure 3. Effectiveness versus number of pairing levels for the case of same volume.

The figure 2 shows that NTU for CHE is more than NHE which implies that the effectiveness of CHE is more than NHE and this also verified by the effectiveness results in figure 3. As the number of pairing level increases NTU of CHE increases more rapidly than the NTU of NHE hence at higher value of n, effectiveness of CHE is even more than that of NHE.

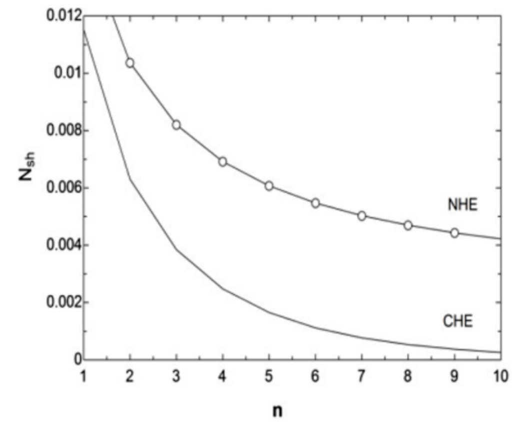

Figure 4. Entropy generation number due to heat transfer versus number of pairing levels for the case of same volume.

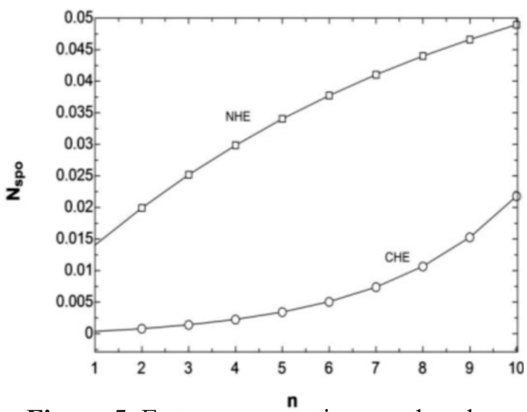

Figure 5. Entropy generation number due to pressure drop versus number of pairing levels for the case of same volume.

Results from figure 4 indicates that the heat transfer entropy generation number for CHE is less than NHE for a given value of number of pairing level n and its value keeps on decreasing for both CHE and NHE as value of n increases. Higher value of heat transfer entropy generation number corresponds to condition of higher losses due to heat transfer irreversiblities. Hence CHE is better than NHE. Also the pressure drop entropy generation number for CHE is less than that of NHE indicating that pressure drop is more

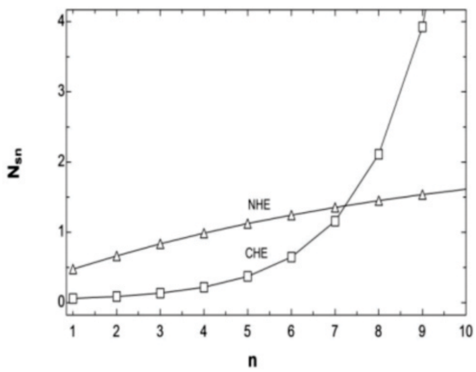

Figure 6. Total entropy generation number versus number of pairing levels for the case of same volume.

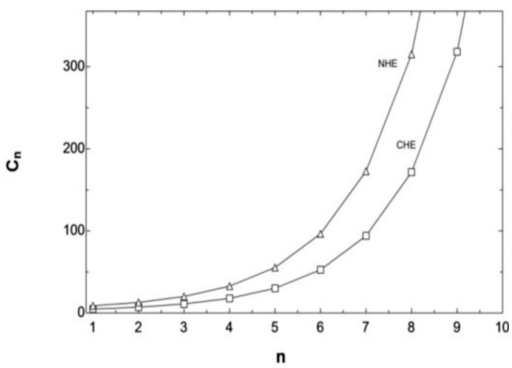

Figure 7. Thermoeconomic cost (total cost) versus number of pairing levels for the case of same volume.

Figure 6 shows that the total entropy generation number for CHE is less than NHE upto pairing level 7 because upto pairing level 7 surface area for CHE is less than that of NHE to achieve same heat transfer rate hence the exergy destruction reduces.

Figure 7 shows that thermoeconomic cost for CHE is less than NHE because of the less material required and also due to less total irreversibility of CHE than NHE.

Case 2: For same surface area between CHE and NHE

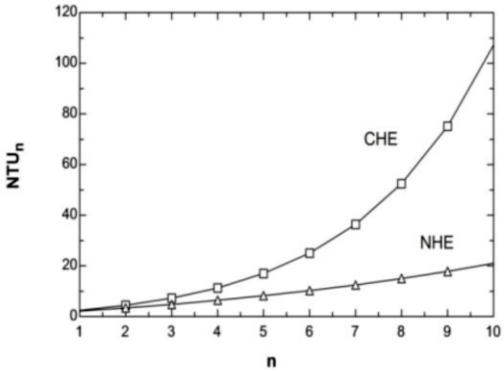

Figure 7. Thermoeconomic cost (total cost) versus number of pairing levels for the case of same volume.

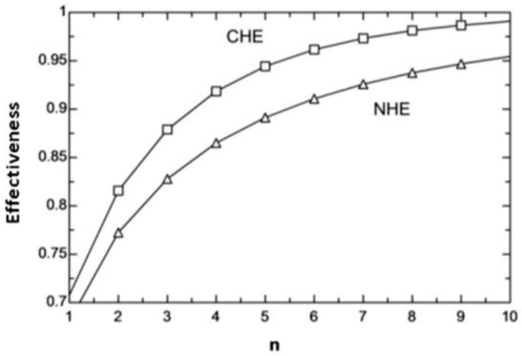

Figure 8. NTU versus number of pairing levels for the case of same surface area.

Same kind of results are obtained in the case 2 as in case 1 which are shown in the figures 8 and 9, i.e. the NTU and effectiveness of CHE is more than NHE except that the difference between the value of NTU or effectiveness for a given paring level is more in this case as compared to case 1.

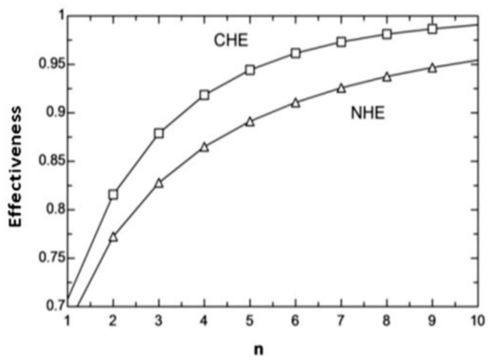

Figure 9. Effectiveness versus number of pairing levels for the case of same surface area.

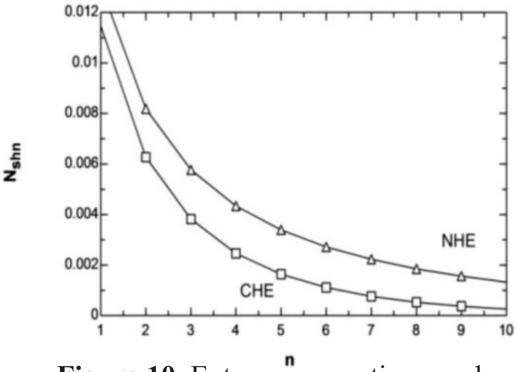

Figure 10. Entropy generation number due to heat transfer versus number of pairing levelsfor the case of same surface area.

As shown in the figure 10, value of heat transfer entropy generation number for CHE is less than NHE for a given value of pairing level signifying less loss due to heat transfer irreversibility. Both the cases shows that a constructal heat exchanger is better than a normal heat exchanger.

Also from the figure 11 that is between pressure drop entropy generation number and pairing level it is clear that in this case too pressure drop is more in case of NHE than CHE. This proves the fact that CHE is designed for minimizing the resistance to fluid flow.

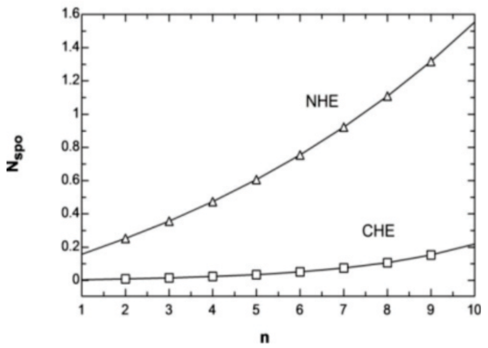

Figure 11. Entropy generation number due to pressure drop versus number of pairing levels for the case of same surface area.

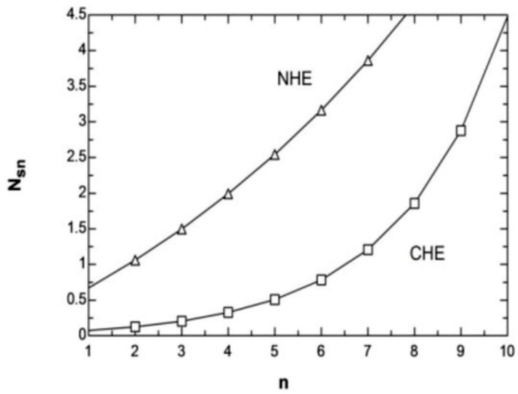

Figure 12. Total entropy generation number versus number of pairing levels for the case of same surface area.

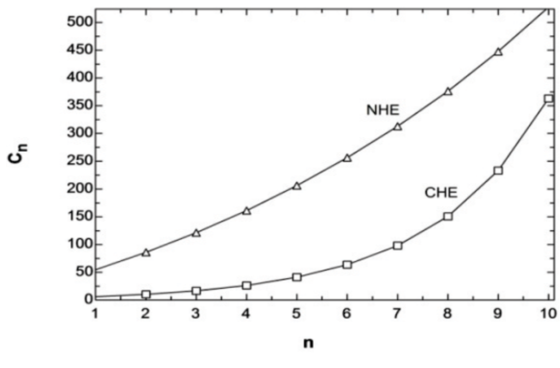

Figure 13. Thermoeconomic cost (total cost) versus number of pairing levels for the case of same surface area.

Figure 12 shows that total entropy generation number for CHE is always less than that of NHE and for no value of pairing level n total irreversiblity of NHE is less than CHE. Figure 13 shows that thermo-economic cost for CHE is less than NHE which proves that CHE is more economical than NHE.

4. **Conclusions**

The following are the conclusions which can be drawn from the analysis. The sum of all irreversibilities that is the total entropy generation number is lower for the CHE as compared to the NHE for a particular value of number of the pairing level and above. However, beyond the value of n=3 the value of total entropy generation number increases significantly.

Total cost (thermoeconomic cost) of heat exchanger also has the same behavior of attaining a minimum value for a particular value of pairing level number which provides an optimum thermoeconomic cost of the CHE for a particular value of the initial length-to-diameter ratio considered.

Also the values of effectiveness and NTU is more for CHE than the NHE. A higher value of effectiveness shows that the particular heat exchanger is more capable of transferring the heat for the same boundary conditions.

From the same surface area case analysis of CHE and NHE, the heat exchanger tubes volume requirement for CHE will be lesser than NHE. This indicates the compactness of CHE under given volume constraint and is applicable to both laminar and turbulent flow cases. This is one of achievements of CHE that it requires lesser heat exchanger material for fabrication.

For the same heat exchanger tube volume between CHE and NHE, the heat exchanger surface area will be more for CHE compared to NHE. This is one of the advantages of CHE which leads to increase in its performance.

From the overall results, we can find that there is an increase in the performance in the CHE compared to the NHE based on second law analysis which leads to conservation of energy.

Nomenclature

A_s	surface area, m^2
A_c	cross-sectional area, m^2
CHE	constructal heat exchanger
c_p	specific heat, j/kg K
D	channel inner diameter, m
f	friction factor
G	mass velocity, kg/m^2 s

h heat transfer coefficient, W/m^2K .

I irreversibility, W

k thermal conductivity, W/m K

L channel length, m

$\dot{m}$ mass flow rate, kg/s

n number of pairing levels

NHE normal heat exchanger

NTU number of heat transfer units

N_s entropy generation number

N_{sh} heat transfer entropy generation number

N_{sp} pressure drop entropy generation number

Nu Nusselt number

P pressure, Pa

ΔP pressure drop, Pa

$\dot{Q}$ heat transfer rate, W

R gas constant, j/kg K

R_e Reynolds number

Sgen entropy generation rate, W/K

St Stanton number

T temperature, K

ΔT temperature difference, K

U overall heat transfer coefficient, W/m^2K

V volume, m^3

Greek symbols

ε effectiveness

μ viscosity, $N\ s/m^2$

ρ density, kg/m^3

Subscripts

c cold stream

h hot stream

i channel rank

in inlet

n for constructal heat exchanger

o for normal heat exchanger

out outlet

r reference condition

References

[1] Bejan A., *Advanced Engineering Thermodynamics*, 2nd ed., New York, Wiley, 1997.

[2] Bejan A., *Shape and Structure, from Engineering to Nature*, Cambridge, UK, Cambridge University Press, 2000.

[3] Bejan A., Lorente S., Constructal theory of generation of configuration in nature and engineering, *J. of Applied Physics* 100, 041301, 2006.

[4] Bejan A., Lorente S., The constructal law and the evolution of design in nature. *Physics of Life Reviews* 8, 209-240, 2011.

[5] Bejan A., Lorente S., Constructal law of design and evolution: Physics, biology, technology and society, *J. of Applied Physics*, 113, 151301, 2013.

[6] Bejan A., Dendritic constructal

heat exchanger with small-scale cross flows and larger-scales counterflows, *Int. J. of Heat and Mass Transfer* 45, 4607–4620, 2002.

[7] Chen Y.P., Cheng P., Heat transfer and pressure drop in fractal tree-like microchannel nets, *Int. J. of Heat and Mass Transfer* 45, 2643–2648, 2002.

[8] Zamfirescu C., Bejan A., Constructal tree-shaped two-phase flow for cooling a surface, Int. *J. Heat and Mass Transfer* 46, 2785–2797, 2003.

[9] Bonjour J., Rocha L. A. O., Bejan A., Dendritic fins optimization for a coaxial two-stream heat exchanger, *Int. J. Heat and Mass Transfer* 47, 111–124, 2003.

[10] da Silva A. K., Lorente S., Bejan A., Constructal multi-scale tree-shaped heat exchanger, *J. Appl. Physics* 96, 1709–1718, 2004.

[11] Muzychka Y. S., Constructal design of force convection cooled microchannel heat sinks and heat exchangers, *Int. J. Heat and Mass Transfer* 48, 3119–3127, 2005.

[12] Raja V. A. P., Basak T., Das S. K., Heat transfer and fluid flow in a constructal heat exchanger. *Proceedings of 15th International Conference on Enhanced, Compact and Ultra-Compact Heat Exchangers: Science, Engineering and Technology*, Whistler, Canada: 147–153, Sept. 11–16, 2005.

[13] Zimparov V., da Silva A. K., Bejan A., Constructal tree-shaped parallel flow heat exchangers, *Int. J. of Heat and Mass Transfer* 49, 4558–4566, 2006.

[14] Zimparov V., da Silva A. K., Bejan A., Thermodynamic optimization of tree-shaped flow geometries, *Int. J. of Heat and Mass Transfer* 49, 1619–1630, 2006.

[15] Zimparov V, da Silva A. K., Bejan A., Thermodynamic optimization of tree-shaped flow geometries with constant channel wall temperature, *Int. J. of Heat and Mass Transfer* 49, 4839–4849, 2006.

[16] Raja V. A. P. Arun P., Basak T., Das S. K., Thermal performance of a multi-block heat exchanger designed on the basis of Bejan's constructal theory. *Int. J. of Heat and Mass Transfer* 51, 3582–3594, 2008.

[17] Miguel A. F., Dendritic structures for fluid flow: Laminar, turbulent and

constructal design. *J. of Fluids and Structure* 26, 330–335, 2010.

[18] Kim Y., Lorente S., Bejan A., Constructal multi-tube configuration for natural and forced convection in cross-flow, *Int. J. of Heat and Mass Transfer* 53, 5121–5128, 2010.

[19] Daguenet-Frick X., Bonjour J., Revellin R., Constructal Microchannel Network for Flow Boiling in a Disc-Shaped Body. *IEEE Trans. on components and packaging tech*. 33, 115-126, 2010.

[20] Zhang C., Chen Y., Wu R., Shi M., Flow boiling in constructal tree-shaped minichannel network, *Int. J. of Heat and Mass Transfer* 54, 202–209, 2010.

[21] Azad A.V., Amidpour M., Economic optimization of shell and tube heat exchanger based on constructal theory, *Energy* 36, 1087–1096, 2011.

[22] Kim Y., Lorente S., Bejan A., Steam generator structure: Continuous model and constructal design, *Int. J. Energy Res*. 35: 336–345, 2011.

[23] Hajmohammadi M.R., Shirani E., Salimpour M.R., Campo A., Constructal placement of unequal heat sources on a plate cooled by laminar forced convection. *Int. J. of Thermal Sciences* 60, 13-22, 2012.

[24] Awad M.M., Muzychka Y.S., *Thermodynamic Optimization, Heat Exchangers - Basics Design Applications*, Dr. Jovan Mitrovic (Ed.), ISBN: 978-953-51-0278-6, InTech, DOI: 10.5772/34711., 2012.

[25] Lee J., Kim Y., Lorente S., Bejan A., Constructal design of a comb-like channel network for self-healing and self-cooling. *Int. J. of Heat and Mass Transfer* 66, 898–905, 2013.

[26] Lorente S., Lee J., Kim Y., Bejan A., Power from a hot gas stream with multiple superheaters and reheaters, *Int. J. of Heat and Mass Transfer* 67, 153–158, 2013.

[27] Manjunath K. Second law analysis of constructal heat exchangers, *Int. Conference on Smart Technologies for Mechanical Engg.*, ISBN: 978-93-83083-35-0, DTU, Delhi, 962-969, October 25-26, 2013.

[28] Hajmohammadi M.R., Nourazar S.S., Campo A., Poozesh S., Optimal discrete distribution of heat flux elements for in-tube

laminar forced convection, *Int. J. of Heat and Fluid Flow* 40, 89–96, 2013.

[29] Hajmohammadi M.R., Poozesh S., Rahmani M., Campo A., Heat transfer improvement due to the imposition of non-uniform wall heating for in-tube laminar forced convection, *Applied Thermal Engg*. 61, 268-277, 2013.

[30] Bejan A., Lorente S., Kim Y., Lee J., Power from a hot gas stream with superheater and reheater in parallel, *Int. J. of Heat and Mass Transfer* 73, 29–32, 2014.

[31] Errera M.R., Lorente S., Bejan A., Assemblies of heat pumps served by a single underground heat exchanger. *Int. J. of Heat and Mass Transfer* 75, 327–336, 2014.

[32] Manjunath K., Kaushik S. C., Second law analysis of unbalanced constructal heat exchanger, *Int. J. of Green Energy* 11, 173-192, 2014.

[33] Manjunath K., Kaushik S. C., Second law analysis of unbalanced constructal heat exchanger, *Int. J. of Green Energy* 11, 173-192, 2014.

[34] Manjunath K., Kaushik S. C., Entropy generation and thermo-economic analysis of constructal heat exchanger, *Heat Transfer – Asian Research* 43, 39-60, 2014.

[35] Manjunath K., Kaushik S. C., Second Law Thermodynamic study of heat exchangers: A Review, *Renewable & Sustainable Energy Reviews* 40, 348–374, 2014.

[36] Bejan A., The concept of irreversibility in heat exchanger design: counter flow heat exchangers for gas-to-gas applications, *J. Heat Transfer* 99, 374–380, 1977.

[37] Wechsatol W., Lorente S., Bejan A., Tree-shaped flow structures with local junction losses, *Int. J. of Heat and Mass Transfer* 49, 2957–2964, 2006.

[38] Shah R.K., Sekulic D.P., *Fundamentals of heat exchangers*, New York, Wiley, 2003.

[39] Bejan, A., *Convection heat transfer* (3rd ed.). Hoboken, NJ, Wiley, 2004.

[40] Holman JP., *Heat transfer,* McGraw-Hill, 2002.

[41] Klein SA., EES - engineering equation solver, version 8.158., F Chart Software, 2008.

Heat Transfer in Microchannel Heat Sink: Review

Sunny Chandra
Mechanical Engineering Department, Research Scholar, N.I.T Patna
sunnychandra27@gmail.com

Om Prakash
Mechanical Engineering Department, Professor, N.I.T Patna
om.prakash@nitp.ac.in

Abstract
High performance computers, avionics, defense systems require powerful cooling systems like micro-channel heat sink to dissipate large amount of heat flux. The microchannel heat sink is usually made from high thermal conductivity materials with the high surface area to have high heat transfer with lower temperature differences. Micro-channelsfabricatedto have high surface area by micro-machining technology. The heat sink features flow boiling of working fluid through a series of parallel micro-channels with cross- sectional dimensions ranging from 10 to 100 µm. The objective of this paper is collectively present the work done by different researchers on the heat transfer mechanism in microchannel heat sink in laminar flow conditions. Two phase heat transfer in microchannel heat sink is more effective than single phase heat transfer as two phase heat sinks dissipates high heat fluxes at smaller flow rate of working fluid in comparison to single phase heat sinks at same temperature difference. Effect of variation of two phase heat transfer coefficient with Reynolds number (Re) and aspect ratio (β) is presented in this paper. Two phase heat transfer coefficient shows increasing trend with Reynolds number and aspect ratio.

Keywords- *Microchannel heat sink; Heat transfer mechanism in microchannel heat sink; two phase heat transfer coefficient.*

Introduction

Due to the faster signal speed and superior performance of electronic devices, the past two decades have witnessed exceptional increases in heat dissipation in high performance computers, electrical vehicle power electronics, avionics, and directed energy laser and microwave weapon systems. Today localized heat dissipation from advanced microprocessors has already exceeded 100 W/cm2, while high-end defence application such as lasers, microwave devices and radars are beginning to exceed 1000 W/cm2, whereas in nuclear reactors needs heat flux removal rate of 10000 W/cm2 [1]. Requirement for heat dissipation will continue to rise with the improvement in technologies and further reduction in the size of these applications. Heat fluxes for different applications are shown in figure 1. Trends of cooling technologies adopted to meet the steep increase in heat fluxes over the years are shown in figure 2. The exponential curve shows the increase in the heat flux and changes in the cooling technologies. Powerful cooling systems are needed to face the challenges of emerging technologies as well as to make possible further developments in these technologies that will increase the heat dissipation. Various cooling systems have been developed to achieve the desired. These consist of pool boiling thermosyphons, channel flow boiling, jet and sprays etc [2]. The concept of micro-channel heat sink was first introduced by Tuckerman and Pease in the early 1980s. Micro-channel heat sink is an inventive cooling technology which removes large heat fluxes from a small volume. The heat sink is usually made from high thermal conductivity materials such as silicon or copper with the micro-channels made-up into its surface by either precision machining or micro-fabrication technology. Micro-channels have characteristics dimensions ranging from 10 to 1000 μm [3] and they serve as flow passages for the working fluid. Very high surface area to volume ratio, large convective heat transfer coefficient, small mass and volume, and small coolant inventory make heat sink very suitable for cooling devices like microprocessors, laser diode arrays, radars, and high-energy-laser mirrors [4]. Micro-channel heat sinks can be categorised as single phase and two phase. The coolant may maintain its liquid single phase state throughout micro-channels for a fixed dissipative heat flux and high flow rate which corresponds to a single-phase heat sink. If coolant flow rate is comparatively low, the liquid coolant may reach its boiling point while flowing in micro-channels and flow boiling occurs, which results in a two-phase heat sink. Two phase heat sinks are ideally suited for dissipating large amount of heat within very limited space which is demand of the modern applications. These devices are light weight and compact, and needs very small coolant inventory.

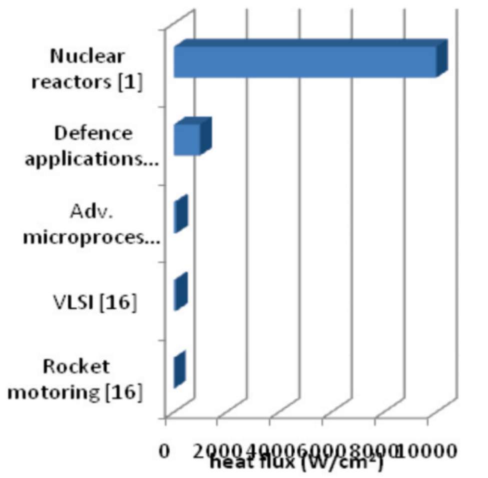

Figure 1: Variation of dissipation of heat flux for different applications

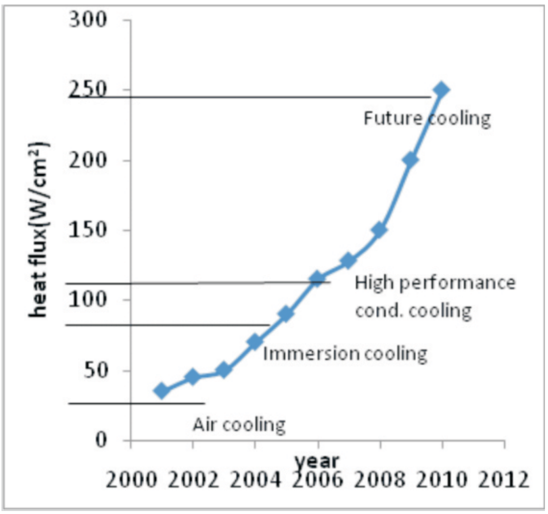

Figure 2: Variation of cooling of Heat flux with year required due to development of new technology in different fields [16].

Abbreviations

W	:	Width of copper block (cm)
L	:	Length of copper block (cm)
W_{ch}	:	Width of microchannels (m)
H_{ch}	:	Height of microchannels (m)
W_w	:	Width of wall separating the microchannels (m)
D_h	:	Hydraulic diameter (m)
T_w	:	Maximum wall temperature at the channel outlet (°C)
h_t	:	Two phase heat transfer coefficient (W/m^2K)
A_{ch}	:	Area of microchannel (m^2)
Nu_3	:	Nusselt number for laminar fullydeveloped flow for three wall heat transfer
Nu_4	:	Nusselt number for laminar fullydeveloped flow for four wall heat transfer
β	:	Aspect ratio

The objective of this paper is to understand the heat transfer phenomena in microchannel heat sink by presenting a review on the different parameters which affects two phase heat transfer coefficient in microchannel heat sink under laminar flow condition.

2. Heat transfer in micro-channel heat sink

Heat transfer mechanism in micro-channel heat sink is different for subcooled and saturated boiling conditions because of the void fractions. In subcooled boiling liquid flow is abundant phase change happens mostly by bubble formation at the wall, while saturated flow boiling in microchannels is governed by two mechanisms: nucleate boiling and forced convection boiling [3]. In the nucleate boiling dominant region, liquid near the heated channel wall is superheated to an adequate degree to maintain the nucleation and growth of vapour bubbles. The heat transfer coefficient in this region is dependent upon heat flux, but less susceptible to mass velocity and vapour quality. The nucleate boiling region is normally related with the bubbly and slug flow patterns, and the forced convection boiling region related to the annular flow pattern. Qu &Mudawar [5] measured the incipient boiling heat flux in a heat sink containing 21 rectangular micro-channels 231 µm wide and 713 µm. Tests were performed with deionized water as coolant at inlet velocities of 0.133-1.44 m/s, inlet temperatures of 30, 60 & 90oC at an outlet pressure of 1.2 bar. Their findings were that at incipient boiling, a small number of nucleation sites appear at the same time close to the exit of several micro-channels, with one or two sites per micro-channel. In the forced convection boiling dominant region, large heat transfer coefficient causes suppression of bubble nucleation along the heated wall, so the heat is transferred mainly by single-phase convection through the thin annular liquid film and carried away by evaporation at the liquid–vapor interface. Qu &Mudawar [3] tested the heat transfer characteristics at a mass velocity range of 135-402 kg/m2s, inlet temperatures of 300C, 600C, and at outlet pressure of 1.17 bar. Results indicated an unexpected transition to annular flow near the point of zero thermodynamic equilibrium quality, and exposed that dominant heat transfer mechanism is forced convective boiling corresponding to annular flow. The heat transfer coefficient in this region depends on coolant mass velocity and vapour quality, but independent of heat flux.Saisorn et al. [6] has studied experimentally the heat transfer characteristics of air–water flow in horizontal micro-channels. The tests were performed at a heat load of 80 W, with superficial Reynolds numbers of gas and liquid ranging between 54–142 and 131–373, respectively. Two inlet sections with different designs were used in this work to investigate the dependency of Nusselt number on flow characteristics. The experiments exposed that the development of small gas slugs instead of gas core flow involves an increase in Nusselt numbers due to which gas–liquid flow gave heat transfer enhancement up to 80% over the liquid flow.Mirmanto [7] performed experiments to investigate local heat transfer coefficients during flow boiling of water in a rectangular microchannel. The hydraulic diameter of the channel was 0.635 mm. The nominal mass fluxes varied from 200 to 700 kg/m2s and heat fluxes in the range of 171 to 685 kW/m2 were applied. An inlet fluid temperature of 98 °C and pressure of 125 kPa were maintained at the microchannel entrance. Results showed that heat transfer is dominated by nucleate boiling and the effect of quality suppresses the local heat transfer coefficient.

2.1 Effect of working fluid other than water on heat transfer performance of microchannel heat sink

In most of studies water is used as working fluid but water is not an appropriate working fluid for removing large amounts of heat from electronic devices because of its current carrying capacity and corrosive nature [8]. Now some researchers have moved to Freon based refrigerants like FC-72, FC-77 because of its high dielectric constant due to which these refrigerants can withstand at very high heat fluxes. But Freon's have also some limitations because of its ozone layer depletion rate which is harmful for environment. Hence now a day's some eco-friendly refrigerants like R134a, R123, R410a, HFE-7000, HFE-7100 etc. are employed as coolant in the test module to solve the problems of corrosiveness and ozone layer depletion. Nascimento et al. [9] performed an experimental investigation of a micro-channel heat sink based on flow boiling of R134 in micro-channels. The results showed that the heat-sink average heat transfer coefficient increases with increasing mass velocity for a fixed mean vapour quality. Dong et al. [10] investigated flow boiling of Freon R141b in rectangular microchannel heat sinks. Experiments were performed over mass velocities ranging from 400 to 980 kg/m2s and heat flux from 40 to 700 kW/m2, and atmospheric pressure at outlet. The results showed that the mean heat transfer coefficient of R141b flow boiling in present microchannel heat sinks depends greatly on mass velocity and heat flux.Lee &Mudawar [11] explored the cooling performance of microchannel heat sink using HFE7100 for four different microchannel sizes. Results revealed that heat fluxes in excess of 700 W/cm2 could be managed without burnout.

2.2 Effect of channel and heat sink geometry on heat transfer in micro-channel heat sink

Channel and heat sink geometry plays important role in heat transfer performance analysis of a micro-channel heat sink.Liu et al. [12] studied the heat transfer performance of the high pin fins with the Reynolds number ranging from 60 to 800 using deionized water as working fluid. The studies were carried out for micro square pin fins of 559x 559 μm2 and 445 x 445 μm2 cross-section. They has concluded that heat dissipation rate could reach 2.83 x 106 W/m2 at the flow rate of 57.225 L/h and the surface temperature of 73.40C for 445 x 445 μm2, also heat resistance decreased with increase in pressure drop.Prajapati et al. 2015 [13] compared the flow boiling characteristics of deionized water in three different configurations of micro-channels through experimental investigations. The investigated channel configurations were uniform cross-section, diverging cross-section and segmented finned micro-channels. Experiments have been conducted with subcooled liquid state at the entry and varying coolant mass and heat fluxes. For entire operating conditions, segmented finned channels demonstrate the highest heat transfer coefficient. Peles et al. 2005 [14] investigated experimentally the heat transfer phenomena over a bank of micro pin fins. It has been observed that very low thermal resistances are achievable using a pin fin heat sink as compared tomicro-channel convective flows, therefore heat transfer performance has been improved for the devices using micro pin fins.Deng et al. [15] has compared the flow boiling performance of reentrant microchannels (REEM) and conventional rectangular microchannels (RECM) at the same hydraulic diameter. Comprehensive comparative experiments with two coolants, i.e., deionized water and ethanol, were performed at inlet sub-cooling of 100C and 400C, and mass fluxes of 200–300 kg/m2s. Experimental results showed that the re-entrantmicrochannels present significant rise in two-phase heat transfer in large inlet subcooling cases and moderate to high heat fluxes.

Two phase heat transfer coefficient investigations for different authors has been compared at different Reynolds number (Re) and different aspect ratio (β). In figure 3. two phase heat transfer coefficient result at Re= 200-600 for different investigations

Table 1: Summary of heat transfer investigations

Author	**Dimensions of MCHS**	**Input parameters**	**Contribution**
Qu & Mudawar.[4]	W= 1.0 cm, L= 4.48 cm, Rectangular channels N=21,W_{ch}= 31□□, W_w= 118□□ H_{ch}=713□□	Coolant& Deionized water, Re= 139&1672 q'= 100W/cm^2 and 200 W/cm^2 Investigation& single phase flow	heat transfer characteristics of micro&channel heat sinks can be effectively predicted using Navier&Stokes and energy equations
Qu &Mudawar. [3]	&same&	&same&	The saturated flow boiling heat transfer coefficient is a strong function of mass velocity, and only a weak function of heat flux and thermodynamic equilibrium quality.
Qu &Mudawar [2]	Rectangular channels N=21, W_{ch}= 215:m, W_w= 125:m H_{ch}= 821:m	T_{in}= 30 & 60□ , P_{out}= 1.13 bar, G= 86&368 kg/m^{2}s	The results show that as CHF was approached, flow instabilities induced vapour backflow into the heat sink's upstream plenum
Nascimento et al. [9]	Copper (28 mm □ 25 mm), Rectangular parallel W_{ch}= 100:m, W_w= 200 :m, H_{ch}= 500:m, N=50	Coolant& R134a G=400&1500 kg/m^{2}s, q'= upto 310 kW/m^2, saturation temperature at outlet = 25□	heat&sink averaged heat transfer coefficient increases with increasing mass velocity for a fixed mean vapour quality.
Saisorn et al. [6]	Rectangular channels W_{ch}=450:m,W_w= 540:m, H_{ch}= 410:m, N= 21,L_{ch}= 40 mm	Q= 80W, Re for gas= 54&142, Re for liquid= 131&373	The gas–liquid flow gave heat transfer enhancement up to 80% over the liquid flow

Liu et al. [12]	Copper substrate(20 mm □ 20 mm Micro square pin fins of 559 □ 559 :m ^{2} and 445 □ 445 :m ^{2} cross&section.	Coolant&deionized water Re =60&800	heat dissipation rate could reach 2.83 □ 10^{6} W/m^{2} at the flow rate of 57.225 L/h and the surface temperature of 73.4^{0}C for 445 □ 445 :m ^{2}.
Dong et al. [10]	W= 0.5 cm, L = 2 cm Rectangular channels W_{ch}=60 :m, W_{w}= 60 :m, H_{ch}= 200 :m,N= 50	Coolant& R141b G= 400 to 980 kg/m^{2}s and q'= 40 to 700 kW/m^{2}	mean heat transfer coefficient of depends greatly on mass velocity and heat flux.
Mirmanto[7]	copper channel (12 mm × 25 mm × 72 mm.) W_{ch}=1710 :m ,H_{ch}= 390 :m, W_{w}=1190 :m	Coolant&water, G= 200 to 700 kg/m^{2}s q'= 171 to 685 kW/m^{2} T_{in}= 98 °C & p_{in}= 125 kPa	heat transfer is dominated by nucleate boiling and the effect of quality suppresses the local heat transfer coefficient.
Prajapati et al. [13]	Copper(25.7 mm □ 12.02 mm) Rectangular cross& section W_{ch}=400 :m(uniform), 300:m(diverging), 400:m(segmented) W_{w}=400:m (uniform), 524:m (diverging), 400:m(segmented) H_{ch}= 750 :m, N= 12	Coolant& deionized water, G= 100&350 kg/m^{2}s, T_{in}= 30□ , Re= 50&500 q'=10&350kW/m^{2}	highest heat transfer coefficient was observed for segmented finned channels as compared to other two configurations of channels for entire operating conditions.
Lee &Mudawar [11]	Rectangular channels W_{ch}=123.4 :m, 123.4:m, 235.2 :m, 259.9 :m, W_{w}= 84.6 :m, 84.6 :m, 230.3 :m, 205.0 :m, H_{ch}= 304.9 :m, 526.9 :m, 576.8 :m, 1041.3 :m, N= 24, 24, 11, 11	Coolant& HFE&7100, T_{in}= &30□ , 0□ , P_{out}= 1.138 bar, m= 2.0& 5.0 g/s	Heat transfer performance of the micro&channel heat sink can be greatly enhanced by lowering the temperature of coolant entering the heat sink.
Deng et al. [15]	copper block (20 mm x 45 mm)Reentrant porous (convex G shaped) channels N=14, D_{h}=786 :m Cavity size=10& 50 :m	Coolant&deionized water & ethanol, T_{in} subcooled= 10^{0}C & 40^{0}C, G= 200–300 kg/m^{2}s, Re= 200&700	two&phase heat transfer showed Signiant rise in large inlet sub cooling cases and moderate to high heat fluxes for the reentrant channels as compared to con&ventional rectangular channels.
Peles et al. [14]	Silicon substrate, cylindrical pin fins of (1.8 mm wide and 243 :m deep with length 10 mm)	De ionized water Re=200&800 q'=790 W/cm^{2}.	Very high heat fluxes can be dissipated at low wall temperature rise using a microscale pin fin heat sink.

has been plotted. Two phase heat transfer coefficient shows increasing trend with Reynolds number from figure 5. It can be understand that higher aspect ratio is beneficial for dissipating high heat fluxes as increase in Nusselt number ratio of three wall and four wall heat transfer leads to enhancement in two phase heat transfer coefficient.

Result and Conclusions

Heat transfer mechanism in

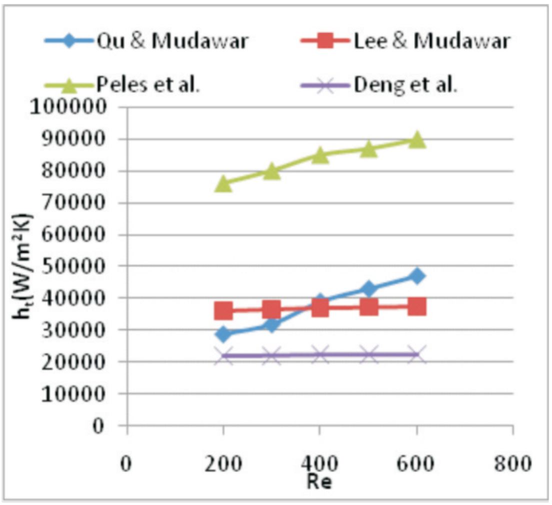

Figure 3: Reynolds number (Re) Vs Two phase heat transfer coefficient (h_t).

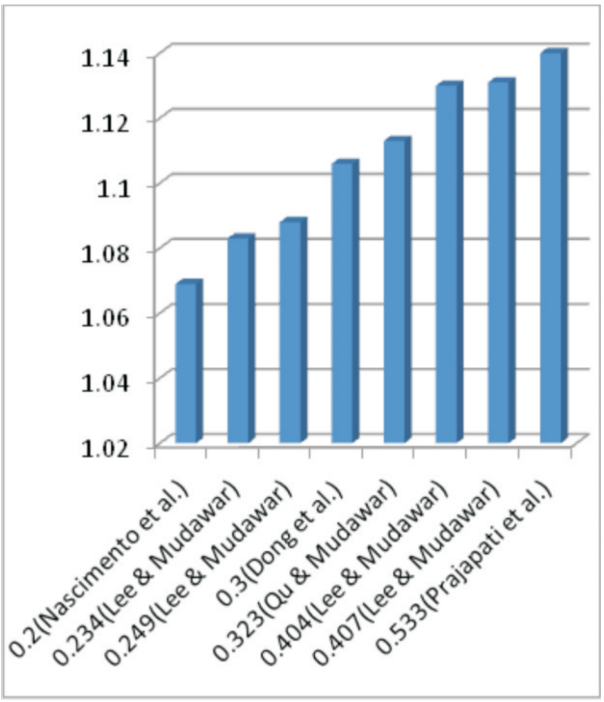

Figure 4: Aspect ratio (β) Vs Nusselt number ratio of three wall and four wall heat transfer $(Nu_3/Nu)_4$

microchannels is different for saturated and subcooled flow boiling conditions. Saturated flow boiling conditions are governed by nucleate and forced convection. The nucleate boiling region is associated with the bubbly and slug flow patterns while forced convection boiling is related to the annular flow. In subcooled flow phase change occurs mostly by bubble formation at the wall.

Two phase heat transfer coefficient enhances with augmentation in Reynolds number (Re) due to which performance of microchannel heat sink will be improved in laminar flow conditions.

Two phase heat transfer coefficient enhances with increase in Nusselt number ratio of three wall and four wall heat transfer due to enhancement in aspect ratio.

From the above review work one can concludes that heat transfer coefficient is having close relation with the Reynolds number but different coefficient of increments. The coefficient of increment is a factor of operating conditions.

References

[1] J. Lee, I. Mudawar, *Fluid flow and heat transfer characteristics of low temperature two-phase micro-channel heat sinks- Part 1: Experimental methods and flow visualization results,* International Journal of Heat and Mass Transfer, vol.51, pp 4315–4326, 2008.

[2] W. Qu & I. Mudawar, *Measurement and correlation of critical heat flux in two-phase micro-channel heat sinks,* International Journal of Heat andMass Transfer, vol. 47, pp 2045–2059, 2004.

[3] W. Qu & I. Mudawar, *Flow boiling heat transfer in two-phase micro-channel heat sinks-I, Experimental investigation and assessment of correlation methods*, International Journal of Heat and Mass Transfer, vol. 46, pp 2755–2771, 2003

[4] W. Qu, I. Mudawar, *Experimental and numerical study of pressure drop and heat transfer in a single-phase micro-channel heat sink,* International Journal of Heat and Mass Transfer, vol. 45, pp

2549–2565, 2002.

[5] W. Qu, I. Mudawar, *Prediction and measurement of incipient boiling heat flux in micro-channel heat sinks,* International Journal of Heat and Mass Transfer, vol. 45, pp 3933–3945, 2002.

[6] S. Saisorn, P. Kuaseng, S. Wongwises, *Heat transfer characteristics of gas–liquid flow in horizontal rectangular micro-channels,* Experimental Thermal and Fluid, vol. 55, pp 54–61, 2014.

[7] M. Mirmanto, *Local pressure measurements and heat transfer coefficients of flow boiling in a rectangular microchannel,*Heat Mass Transfer, vol.52, pp 73-83, 2016.

[8] S.T. Kadam, R. Kumar, *Twenty first century cooling solution: Microchannel heat sinks-A Review,* International Journal of Thermal Sciences, vol. 85, pp 73-92, 2014.

[9] F.J.D Nascimento, H.L.S. Leao, G. Ribatski, *An experimental study on flow boiling heat transfer of R134a in a microchannel-based heat sink,* Experimental Thermal and Fluid Science, vol. 45, pp 117–127, 2013.

[10] T. Dong, Z. Yan, Q. Bi, Y. Zhang, *Freon R141b flow boiling in silicon microchannel heat sinks:* experimental investigation, Heat Mass Transfer, vol. 44, pp 315–324, 2008.

[11] J. Lee, I. Mudawar, *Fluid flow and heat transfer characteristics of low temperature two-phase micro-channel heat sinks- Part 2. Subcooled boiling pressure drop and heat transfer,* International Journal of Heat and Mass Transfer, vol. 51,pp 4327–4341, 2008.

[12] M. Liu, D. Liu, S. Xu, Y. Chen, *Experimental study on liquid flow and heat transfer in micro square pin fin heat sink,* International Journal of Heat and Mass Transfer, vol. 54, pp 5602–5611, 2011.

[13] Y. K. Prajapati, M. Pathak, M. K Khan, *A comparative study of flow boiling heat transfer in three different configurations*

of microchannels, International Journal of Heat and Mass Transfer, vol. 85, pp 711-722, 2015.

[14] Y. Peles, A. Kosar, C. Mishra, C.J Kuo, B. Schneider, *Forced convective heat transfer across a pin fin micro heat sink,* International Journal of Heat and Mass Transfer, vol.48, pp 3615-3627, 2005.

[15] D. Deng, W. Wan, H. Shao, Y. Tang, J. Feng, J. Zeng, *Effects of operation parameters on flowboiling characteristics of heat sink cooling systems with reentrant porous microchannels,* Energy Conversion and Management, vol. 96, pp 340-351, 2015 340–351.

[16] *Thermal Management in Electronic Equipment,* HCL Technologies, February 2010.

Thermal Performance and Emission Test of CI Engine Using Biodiesel Produced from Waste Cooking Oil Blend With Diesel

Jatinder Kataria and S.K. Mohapatra
Department of Mechanical Engineering, Thapar University,
Patiala. Punjab, India,
Jatinder80@gmail.com, skmohapatra@thapar.edu

K. Kundu
Department of Bio fuel, Centre of Excellence for Farm Machinery,
Ludhiana.Punjab, India
K_kundu@cmeri.res.in

Abstract
Compression ignition (C.I.) engine is the undebated choice for power applications, stationary or mobile. There is an urgent need of alternative high potential fuel for C.I. engines in order to fulfil energy needs without hampering the thermal performance and stringent emission standards. In the present work, a four stroke variable compression ratio engine was tested. Waste cooking oil was chosen as an alternative fuel, which was upgraded into biodiesel in the laboratory using mechanical stirring and ultrasonic cavitation technique of biodiesel production. The various biodiesel blends were prepared (i.e. B20, B40, B60, B80 and B100) with conventional diesel fuel and two compression ratios (i.e. 15, 17.5) were chosen for present work. The experimental test rig including hardware interfaced with engine soft software was used for online data logging for thermal performance of engine in tabulated and graphical form. The emission of CO, HC, and NOx were measured using AVL gas analyser (AVL Di gas 444), while smoke opacity was recorded using AVL 437. The thermal and engine emissions were obtained in the laboratory for different concentration of biodiesel blends at two compression ratios (i.e. 15, 17.5) for comparative analysis. The results showed that as the biodiesel concentration in a blend was increased, the thermal performance and emission were observed to be

marginally higher; on the other hand as compression ratio was increased, the thermal performance improved, CO and smoke opacity decreased, while HC and NOx level increased.

Keywords- *Compression ignition engine; waste cooking oil; mechanical stirring; ultrasonic cavitation,; smoke opacity; thermal performance*

Introduction

In the present context, compression ignition engines are the undebated choice for almost all shaft power (stationary or mobile) applications. The massive utilization of diesel fuel due to their superior fuel economy and robustness has resulted in diesel crisis, in addition to environment threat leading to climate change. From a survey, the world consumption for petroleum and other liquid fuels is expected to reach at 107 million barrel per day by 2030 [1]. The globe today uses about 147 trillion kWh of energy which is expected to rise in the coming future [2]. Under such exponentially increasing trend, it can be realized that the petroleum resources might be depleting fast. A major chunk of this exponential rise in energy demand will be due to the developing countries, which is bound to grow leaps and bounds. Another major global concern is environmental degradation. The intergovernmental panel on climate change (IPCC) concluded in “climate change- 2007” that because of global warming effect the global surface temperatures are likely to increase by $1.1C^{0}$ to $6.4C^{0}$ between 1990 and 2100. Due to these two reasons the whole world is in the search of an alternative fuel which is similar to the conventional diesel in terms of physical and chemical properties and can be used in the existing diesel engine without any engine modifications. Biodiesel is biodegradable, renewable and environment- friendly [3].

1.1 Biodiesel Fuel

The idea of utilization of vegetable oil as substitute for diesel was demonstrated by Rudolph Diesel around the year 1900, when vegetable oil was proposed as fuel for engines. Various products derived from vegetable oils have been proposed as an alternative fuel for diesel engines [4]. Biodiesel can be produced from an enormous feedstock such as vegetable oils or animal fats [5].Vegetable oils may be edible or non-edible. Previously, the use of vegetable oil as diesel fuel was limited due to its high viscosity (near 10 times of the gas oil) [6]. In order to adapt the fuel to the existing engine the properties of vegetable oil had to be modified. The increased viscosity and low volatility of vegetable oils for diesel engine lead to severe engine deposits, injector choking and piston ring sticking [7]. However, these effects can be minimised or eliminated through transesterification process of vegetable oil to form methyl ester [8]. Transesterification will reduce the viscosity up to the level of conventional diesel and will make the fuel suitable for engine operations. Transesterification is the process of reacting a triglyceride with an alcohol in the presence of a catalyst to produce glycerol and fatty acid esters. The whole process is shown in fig1

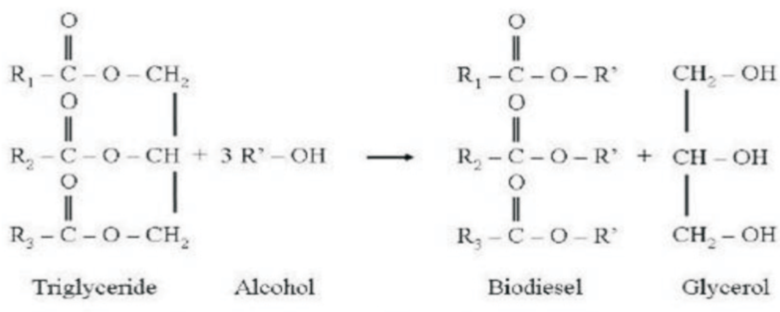

Fig-1. Transesterification Process

ASTM international defines "Biodiesel as the mono alkyl esters of long chain fatty acids derived from renewable liquid feedstock such as vegetable oils and animal fats for use in CI engines". Biodiesel can be blended in any proportions with petroleum diesel or can be used neatly. The use of biodiesel in conventional diesel engines results in substantial reduction in all emissions except NOx which can be controlled by EGR [9]. Biodiesel differs from conventional diesel fuel in its chemical and thermophysical properties which results in the difference in its combustion characteristics. For instance, the cetane number of biodiesel is higher than conventional diesel which leads to the shorter ignition delay time. The viscosity of biodiesel is higher approximately 1.5 times than conventional diesel [10] and due to larger viscosity the combustion duration of biodiesel is higher. On account of high kinematic viscosity; nozzle fuel spray, evaporation and atomization process of biodiesel results in slower burning and longer combustion duration [11], despite the duration is shorter than conventional diesel under low, medium and high load [12]. The cold flow properties such as cloud point and the pour point are also greater than conventional diesel. Due to this, it is less responsive in cold weather which results in difficult starting in cold weather. The heat release rate of biodiesel is lower than conventional diesel, lessening the peak pressure rise rate, peak cylinder pressure and power. It is estimated that in current scenario, as compared to conventional diesel the cost of biodiesel is higher, which is the main hindrance to its commercialization. 70%-85% of the total biodiesel production cost arises from the cost of raw material [13]. Using waste cooking oil as raw material should reduce the raw material cost and make it competitive in price with conventional diesel. Waste cooking oil thus opened a good opportunity to study its suitability to produce biodiesel. Thus the main aim of this work was to investigate the physical and chemical characteristics of waste cooking oil and compare these properties with base line diesel for thermal and emission performance. The properties of the base line diesel and waste cooking methyl ester are given in table 1.

2. Experimental Setup

Experimental setup consisted of

variable compression ratio compression ignition engine of 3.5 kW rated power single cylinder vertical water cooled engine connected to eddy current dynamometer for loading. This setup enabled varying the compression ratio for measurement of engine's thermal performance parameters (i.e., brake power, indicated power, frictional power, BMEP, IMEP, brake thermal efficiency, indicated thermal efficiency, mechanical efficiency, volumetric efficiency, specific fuel consumption, A/F ratio) using engine performance analysis software package "Engine Soft LV". A set of piezoelectric sensors were mounted on the engine for pressure measurements. One mounted on cylinder head, was for measuring cylinder pressure and the other was mounted on the fuel line near the injector for measuring injection pressure. The piezo sensors have an advantage of good frequency response and linear operating range. Specially designed tilting cylinder block arrangement mechanism was used for varying the compression ratio without stopping the engine and without altering the combustion chamber geometry. The compression ratio could not be brought below 13 because of knocking and greater vibration. A small water pump was

Table-1. Properties of diesel and waste cooking oil methyl ester

Item	Units	ASTM STANDARDS	DIESEL	Biodiesel	ASTM Methods
Cetane Number	**--**	**--**	**50.88**	**51.34**	**ASTM D 4737**
Lower Heating value	**MJ/Kg**	**--**	**42.98**	**38.85**	**ASTM D3338**
Density	**kg/m^3**		**820**	**878**	**ASTM D 1298**
Kinematic Viscosity	**cst**	**<5**	**2.049**	**3.57**	**ASTM D445**
Flash Point	**C**	**>130**	**60**	**90**	**ASTM D93**
Fire Point	**C**	**>53**	**67**	**150**	**---------**
Calorific value	**kJ/kg**	**>33000**	**42000**	**39543**	**-------------------**

used for continuous flow of water for cooling the engine and its associated parts. An eddy current dynamometer was used for loading the engine. The dynamometer consisted of a rotor mounted on a shaft running in bearings, which rotates within a casing. Inside the casing, there were two field coils connected in series. When these coils were supplied with a direct current, a magnetic field was created in the casing on either side of the rotor. When the rotor was turned in this magnetic field, eddy currents were induced creating a braking effect between the rotor and casing. The rotational torque exerted on the casing was measured by a strain gauge load cell incorporated in the restraining linkage between the casing and dynamometer bedplate. To prevent overheating of the dynamometer, water was circulated through the casing using a pump. The setup consisted of transmitters for air and fuel flow measurements. Rota meters were provided for cooling water and calorimeter water flow measurement. Provision was also made for online measurement of temperature of exhaust, inlet, and outlet cooling water and calorimeter water flow rate and load on the engine. These signals were interfaced to a computer through a data acquisition system. Windows based engine performance analysis software package "Engine soft LV" was used for online performance evaluation. The software displays P- ω and P-V diagrams, power, mean effective pressure, thermal efficiency, specific fuel consumption, air-fuel ratio, and heat utilized. The exhaust gases from the engine were sampled from exhaust line through a specially designed arrangement for diverting the exhaust gas through sample line without increasing the back pressure and was then analysed using exhaust gas analyser. The gases measured were CO (% and ppm), CO_2 (%), HC (ppm), O_2 (%), NOx (ppm), and SOx (ppm). For measurement of smoke intensity of the exhaust gas, a smoke meter was used. The smoke intensity was measured in terms of Hartridge Smoke Unit (%). The instrument also measured the absorption coefficient K of the exhaust gas in m^{-1}.The specifications of the engine used for conducting the experiments are as given in Table 2.

3. Experımental Procedure

The experiment was conducted for pure diesel, blends of biodiesel from waste cooking oil with diesel and, pure biodiesel from waste cooking oil which is termed as B100. BXX is the general term used for blend where XX signifies the percentage of biodiesel in the

Table-2. Test Engine Specification

Engine Type	**Variable compression ratio 4 stroke Compression ignition engine**
Number of cylinders	One
Bore and stroke	87.5 X 110 mm
Compression ratio	12 to 18
Swept volume	661cc
Rated power	3.5 kW @ 1500 rpm
Fuel injection timing	24^0 BTDC
Type of injection nozzle	Pintle
Number of nozzle	01
Nozzle hole diameter	0.25 mm

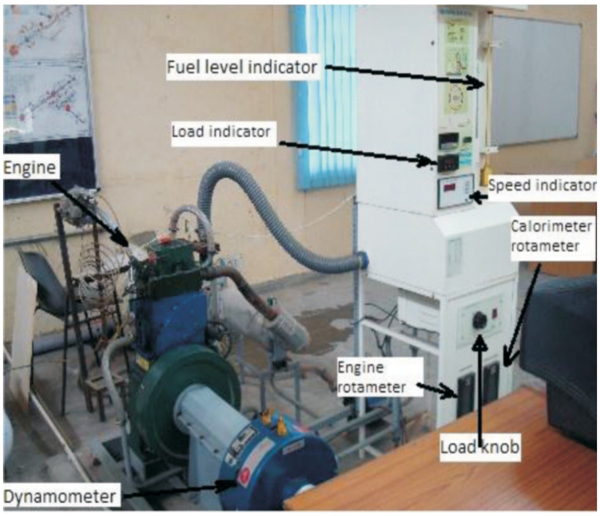

Fig-2. Photographic view of VCR CI Engine blend. For example a blend of 20% biodiesel and 80% diesel the designation is B20. The experiments were performed for diesel, B20, B40, B60, B80, and B100. Before cranking the engine, a sufficient amount of lubricating oil and fuel was ensured. The water flow was set at 250 LPH and calorimeter to 60 LPH. The computer was powered ON and ENGINESOFT LV was started and the calorific value, density of fuel and compression ratio were entered. Now the engine was cranked manually and made to run ideally for 5 min. When the engine reached its stabilized conditions, the readings were recorded at different loading conditions such as no load, part load and full load. For changing the compression ratio, tilting cylinder head mechanism was used which is user- friendly. By loosening the Allen bolts, the block was tilted by using the adjuster screw to a particular compression ratio. After attaining the desired compression ratio, the Allen bolt was tightened. The range of compression ratio was varied from 14 to 18 and injection pressure 150 bar to 250 bar.

The thermal performance of the engine was evaluated in terms of brake-specific fuel consumption (BSFC) and brake thermal efficiency (BTHE), and the emissions measured were carbon monoxide, carbon dioxide, unburnt hydrocarbon, oxides of nitrogen, oxides of sulfur, and oxygen. The smoke intensity and absorption coefficient of exhaust gas were also measured.

4. Results and Dıscussıons

Various engine performance parameters such as brake thermal efficiency, specific fuel consumption, mechanical efficiency and engine emission parameters such as carbon monoxide, unburnt hydrocarbon, nitric oxide and smoke opacity were measured at two compression ratios (i.e. 15:1 and 17.5:1) for all blends of biodiesel along with diesel at different engine loads.

4.Brake Specific Fuel Consumption (BSFC)

The effect of variation of brake power output on specific fuel consumption at typical compression ratios of 17.5 and

15 for different biodiesel blends are shown in figure 4.1-4.3. The specific fuel consumption decreases with brake power output. It can be observed that specific fuel consumption does not show any significant deviation with different blends of biodiesel fuel. The effect of compression ratio has been highlighted in fig 3. It shows marginally lower specific fuel consumption at higher compression ratio. It can be observed that for all blends of biodiesel, the brake specific fuel consumption was higher than conventional diesel. This pattern was due to the fact that biodiesel blends have a lower heating value than does conventional diesel. We can also see that the BSFC of B20 is almost the same as that of base line diesel at both compression ratios (17.5 and 15 respectively).

5. Brake Thermal Efficiency

The effect of variation of brake power output on brake thermal efficiency at typical compression ratios of 17.5 and

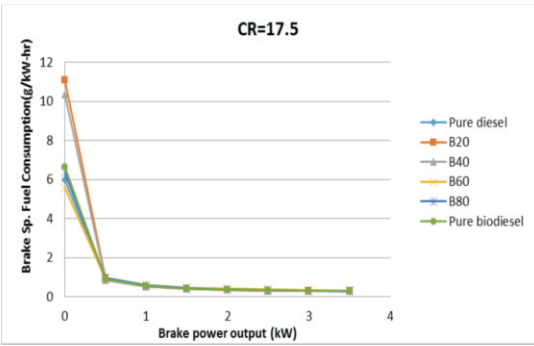

Fig-4.1. Brake specific fuel consumptions v/s Brake power (CR

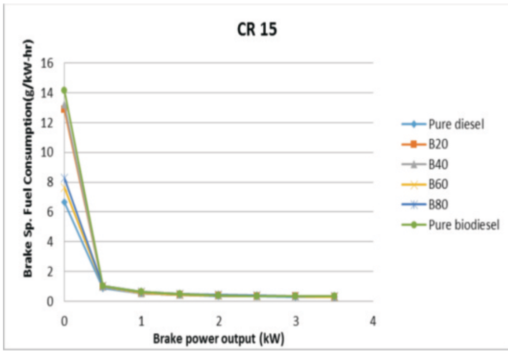

Fig-4.2. Brake specific fuel consumptions v/s Brake power (CR 15)

15 for different biodiesel blends are shown in figures 5.1-5.3. The brake thermal efficiency of the engine increases with brake power output. It can be observed that brake thermal efficiency at different blends is comparable with diesel fuel. For CR of 17.5, the maximum values of brake thermal efficiencies were recorded to be 31.99 and 31.72 for biodiesel

blends of B60 and B80, respectively. At CR values of 17.5 and 15, the maximum value of thermal efficiency was obtained at B20. Similar results were also reported by Ozsezen et al., 2009 [14].

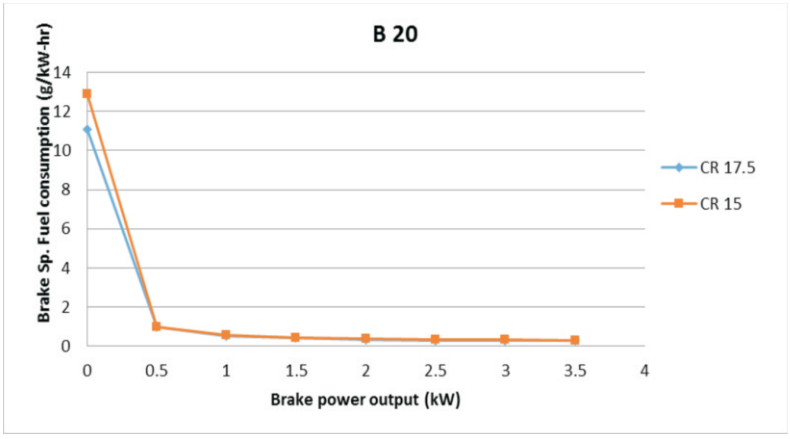

Fig-4.3. Comparison of Brake specific fuel consumptions v/s Brake power CR 17.5 & 15

6. Emission Characteristics

Carbon-monoxide

Carbon monoxide is one of the arbitrate compound formed during the intermediate combustion stage of hydrocarbon fuels. CO formation

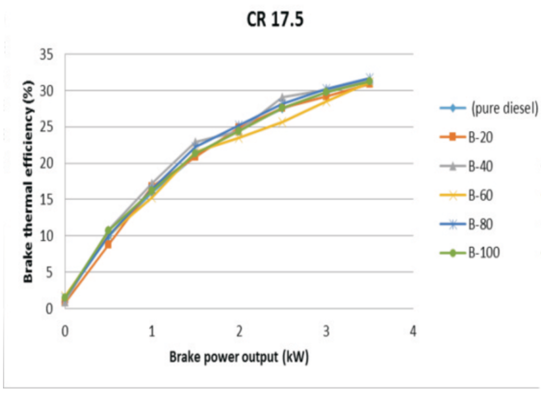

Fig-5.1. Brake thermal efficiency v/s Brake power output CR 17.5

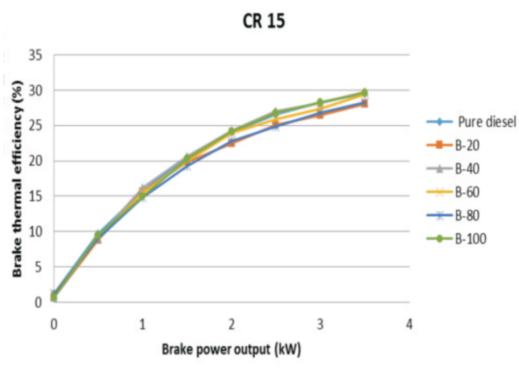

Fig-5.2. Brake thermal efficiency v/s Brake power output CR 15

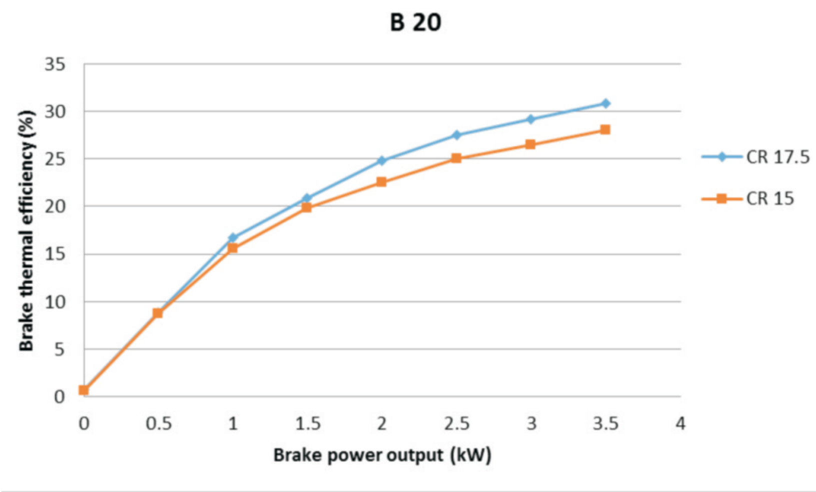

Fig-5.3. Brake thermal efficiency v/s Brake power output CR 17.5,15

depends on air fuel equivalence ratio, fuel type, combustion chamber design, starting of injection timing, injection pressure and speed. The effect of brake power output of engine on carbon-monoxide emission with various blends of biodiesel at two levels of compression ratio (i.e., 17.5 and 15) has been plotted in figure 6.1 and 6.2. At part load, pure diesel mode (with CR of 17.5) shows slightly lower level of CO emission than any biodiesel blends; at full loads, the biodiesel blends show better control on carbon-monoxide emissions. It may be expected due to complete oxidation. However, at CR of 15, the biodiesel shows slightly higher trends for CO emission than pure diesel mode. Similar trends were also accounted by Mazumdar and Agarwal, and Rao et al [15-16].

7. Oxides of Nitrogen Emission

The effect of variation of brake power output on NOx emissions at compression ratios of 17.5 and 15 for different biodiesel blends are shown in figure 7.1 and 7.2. NOx emissions increase with the increase in concentration of biodiesel in the blend and compression ratio. The emissions of nitrogen oxides from engine exhaust are highly dependent on

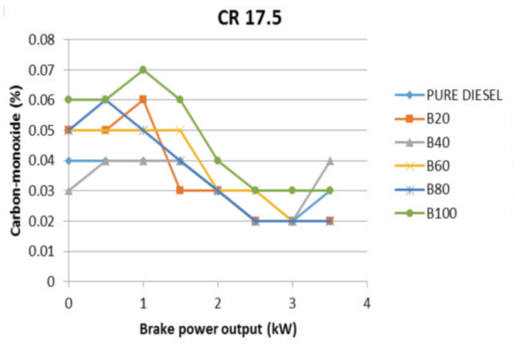

Fig. 6.1. Carbon monoxide v/s Brake power output CR 17.5

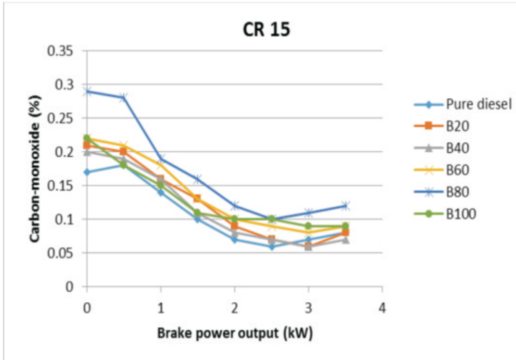

Fig. 6.2. Carbon monoxide v/s Brake power output CR 15

oxygen concentration and thus, the combustion temperature. In general the NOx concentration varies linearly with the load of the engine. As the load increases, the overall fuel-air ratio increases resulting in an increase in the average gas temperature in the combustion chamber and hence NOx formation, which is sensitive to temperature increase. The NO_x obtained in this experiment follows the trends as described by Shirneshan [17].

8. Unburnt Hydro-Carbon Emission

The effect of variation of brake power output on hydrocarbon emissions at compression ratios of 17.5 and 15 for

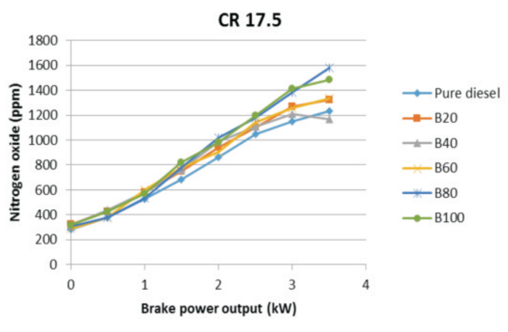

Fig. 7.1. Nitrogrnoxide v/s Brake power output CR 17.5

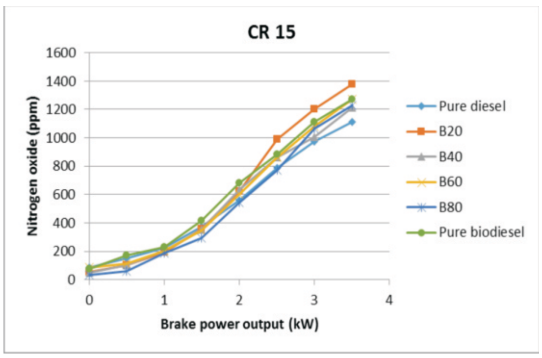

Fig. 7.2. Nitrogrnoxide v/s Brake power output CR 15

different biodiesel blends are shown in figure 8.1 and 8.2**.** The emission of hydrocarbons (HC) tends to decrease with increasing the concentration of biodiesel in the blends as shown in figure. The reduction in the HC was linear with the addition of biodiesel for the blends tested. These reductions indicate a complete combustion of the fuel. Waste cooking oil biodiesel contains high oxygen content, which makes better combustion.

9. Smoke Opacity

The effect of variation of brake power output on smoke opacity at compression ratios of 17.5 and 15 for different biodiesel blends are shown in figure 9.1 and 9.2. Smoke opacity

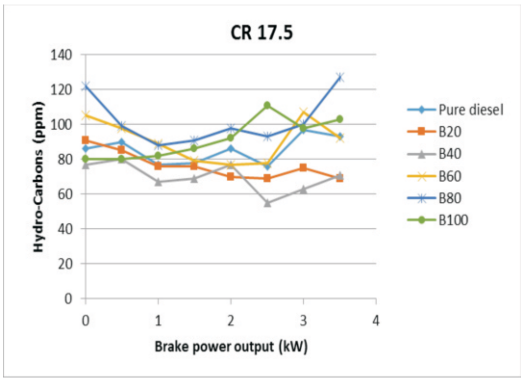

Fig. 8.1. Unburnt hydrocarbon v/s Brake power output CR 17.5

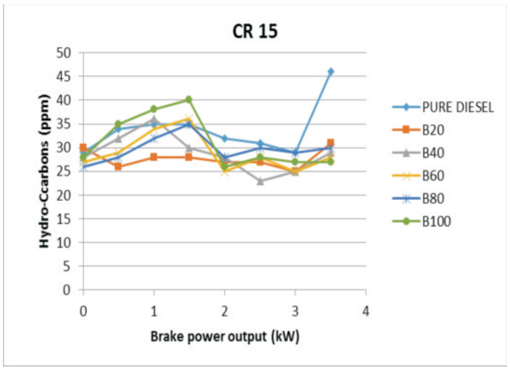

Fig. 8.2. Unburnt hydrocarbon v/s Brake power output CR 15

gives slightly increasing trends with brake power output. However, as either biodiesel concentration or compression ratio increases, the smoke opacity increases.

Conclusions

In the present work, the thermal performance and emission characteristics of a variable compression ratio compression ignition engine fueled with biodiesel produced from waste cooking oil have been experimentally investigated and compared with base line diesel. The final inferences of the present work are summed up as follows.

1. The diesel engine can run

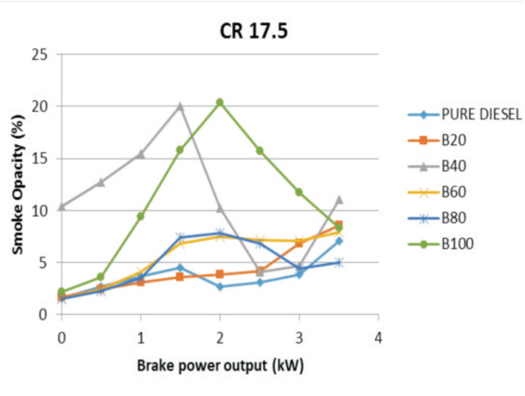

Fig. 9.1. Smoke opacity v/s Brake power output CR 17.5

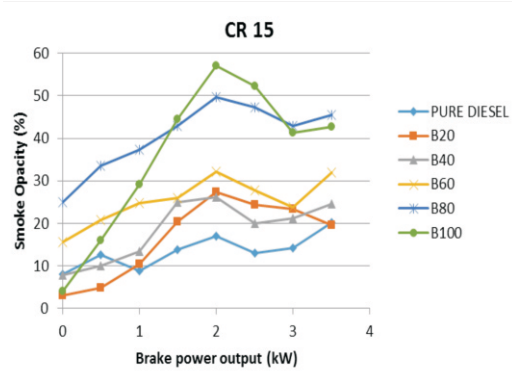

Fig. 9.2. Smoke opacity v/s Brake power output CR 15

satisfactorily on biodiesel and its blends with diesel without any engine modification.

2. The specific fuel consumption decreases with brake power output. The different blends of biodiesel fuel do not put any significant effect on specific fuel consumption. Specific fuel consumption is inversely proportional to compression ratio. It can be observed that for all blends of biodiesel, the brake specific fuel consumption was higher than conventional diesel. This pattern was due to the fact that biodiesel blends have a lower heating value than conventional diesel.

3. There is significant reduction in CO, unburnt hydrocarbons and smoke emissions for biodiesel and its blends as compared to conventional diesel. Whereas, NOx emission of waste cooking oil methyl esters is marginally higher than conventional diesel.

It can be summed up that in order to minimize the dependency on fossil fuels, waste cooking oil methyl ester is competent enough as conventional diesel, which will solve the problem of air pollution and utilization of waste cooking oil (by trans- esterifying it to produce biodiesel for compression ignition engine)

References

[1] Intergovernmental Panel. "IPCC Fourth Assessment Report on Climate Change", 2009.

[2] Energy Information administration. "International Energy Outlook", Office of Integrated Analysis and Forecasting, U.S. Department of Energy, (2009).

[3] H. An, W.M. Yang, A. Maghbouli, J. Li, S.K. Chou, K.J. Chua. Performance, combustion and emission characteristics of biodiesel derived from waste cooking oil. Applied Energy 2013; 112: 493–499.

[4] Ministry of Petroleum and Natural gas, "Government of India", April 20, 2009.

[5] V. Bhardwaj, S. Sharma, S. K. Mohapatra, K. Kundu. Performance and emission characteristics of a C.I. engine fuelled with different blends of biodiesel derived from mustard oil. Proceedings of International Conference on Advances in Mechanical Engineering 2013 80-86.

[6] A. K. Agarwal. Biofuels (alcohols and biodiesel) applications as fuels for internal combustion engines. Progress in Energy and Combustion Science 2007; 33: 233–271.

[7] G. Velgutth. 1983. Performance of vegetable oil and their monsters as fuel for diesel engine. Society of Automotive Engineers 1983; Paper Number 831358.

[8] S.J. Clark, L. Wagner, M. D. Schrock, P.G. Piennar. Methyl and ethyl soybean esters as renewable fuels for diesel engine. Journal of the American Oil Chemists Society 1984; 61(10) 1632–1638.

[9] D. Agarwal, S. Sinha, A. K. Agarwal. 2006. Experimental investigation of control of Nox emissions in biodiesel fuelled compression ignition engine. Renewable Energy 2006; 31:

2356–2369.

[10] J.F. Sun, JA. Caton. TJ. Jacobs. 2010. Oxides of nitrogen emissions from biodiesel fuelled diesel engine. Progressive Energy Combustion Science 2010; 36: 677–95.

[11] L. Raslavicius and Z. Bazaras. Variation in oxygenated blend composition to meet energy and combustion characteristics very similar to diesel fuel. Fuel Process Technology 2010; 91: 1049-54.

[12] J. Bittle, B. Knight, T. Jacobs. 2009 The impact of biodiesel on injection timing and pulse width in a common rail medium-duty engine. Presented at the SAE power train fuels and lubricants fall meeting. San Antonio Texas SAE 01-2782.

[13] X. Meng, G. Chen, Y. Wang. Biodiesel production from waste cooking oil via alkali catalyst and its engine test. Fuel Process Technology 2008; 89: 851–857.

[14] A. N. Ozsezen, M. Canakci, A. Turkcan, C. Sayin. Performance and combustion characteristics of a DI diesel engine fuelled with waste palm oil and canola oil methyl esters. Fuel 2009; 88: 629-636.

[15] B. Mazumdar, A. K. Agarwal. Performance emission and combustion characteristics of biodiesel (Waste cooking oil methyl ester) fuelled IDI engine. Society of Automotive Engineers 2008; 01–13.

[16] G. L. N. Rao, S. Sampath, K. Rajgopal. Experimental studies on the combustion and emission characteristics of a diesel engine fuelled with used cooking oil methyl ester and its diesel blends. International Journal of Engineering and Applied Science 2008; 4: 64–70.

[17] A. Shirneshan. HC, CO, CO_2 and NOx emission evaluation of a diesel engine fuelled with waste frying oil methyl ester 2013; 75: 292–297.

Instructions for Authors

Essentials for Publishing in this Journal

- Submitted articles should not have been previously published or be currently under consideration for publication elsewhere.
- Conference papers may only be submitted if the paper has been completely re written (taken to mean more than 50%) and the author has cleared any necessary permission with the copyright owner if it has been previously copyrighted.
- All our articles are refereed through a double-blind process.
- All authors must declare they have read and agreed to the content of the submitted article and must sign a declaration correspond to the originality of the article.

Submission Process

All articles for this journal must be submitted using our online submissions system. http://enrichedpub.com/ . Please use the Submit Your Article link in the Author Service area.

Manuscript Guidelines

The instructions to authors about the article preparation for publication in the Manuscripts are submitted online, through the e-Ur (Electronic editing) system, developed by **Enriched Publications Pvt. Ltd**. The article should contain the abstract with keywords, introduction, body, conclusion, references and the summary in English language (without heading and subheading enumeration). The article length should not exceed 16 pages of A4 paper format.

Title

The title should be informative. It is in both Journal's and author's best interest to use terms suitable. For indexing and word search. If there are no such terms in the title, the author is strongly advised to add a subtitle. The title should be given in English as well. The titles precede the abstract and the summary in an appropriate language.

Letterhead Title

The letterhead title is given at a top of each page for easier identification of article copies in an Electronic form in particular. It contains the author's surname and first name initial .article title, journal title and collation (year, volume, and issue, first and last page). The journal and article titles can be given in a shortened form.

Author's Name

Full name(s) of author(s) should be used. It is advisable to give the middle initial. Names are given in their original form.

Contact Details

The postal address or the e-mail address of the author (usually of the first one if there are more Authors) is given in the footnote at the bottom of the first page.

Type of Articles

Classification of articles is a duty of the editorial staff and is of special importance. Referees and the members of the editorial staff, or section editors, can propose a category, but the editor-in-chief has the sole responsibility for their classification. Journal articles are classified as follows:

Scientific Articles:

1. Original scientific paper (giving the previously unpublished results of the author's own research based on management methods).
2. Survey paper (giving an original, detailed and critical view of a research problem or an area to which the author has made a contribution visible through his self-citation);
3. Short or preliminary communication (original management paper of full format but of a smaller extent or of a preliminary character);
4. Scientific critique or forum (discussion on a particular scientific topic, based exclusively on management argumentation) and commentaries.

   Exceptionally, in particular areas, a scientific paper in the Journal can be in a form of a monograph or a critical edition of scientific data (historical, archival, lexicographic, bibliographic, data survey, etc.) which were unknown or hardly accessible for scientific research.

Professional articles:

1. Professional paper (contribution offering experience useful for improvement of professional practice but not necessarily based on scientific methods);
2. Informative contribution (editorial, commentary, etc.);
3. Review (of a book, software, case study, scientific event, etc.)

Language

The article should be in English. The grammar and style of the article should be of good quality. The systematized text should be without abbreviations (except standard ones).

All measurements must be in SI units. The sequence of formulae is denoted in Arabic numerals in parentheses on the right-hand side.

Abstract and Summary

An abstract is a concise informative presentation of the article content for fast and accurate Evaluation of its relevance. It is both in the Editorial Office's and the author's best interest for an abstract to contain terms often used for indexing and article search. The abstract describes the purpose of the study and the methods, outlines the findings and state the conclusions. A 100- to 250- Word abstract should be placed between the title and the keywords with the body text to follow. Besides an abstract are advised to have a summary in English, at the end of the article, after the Reference list. The summary should be structured and long up to 1/10 of the article length (it is more extensive than the abstract).

Keywords

Keywords are terms or phrases showing adequately the article content for indexing and search purposes. They should be allocated heaving in mind widely accepted international sources (index, dictionary or thesaurus), such as the Web of Science keyword list for science in general. The higher their usage frequency is the better. Up to 10 keywords immediately follow the abstract and the summary, in respective languages.

Acknowledgements

The name and the number of the project or programmed within which the article was realized is given in a separate note at the bottom of the first page together with the name of the institution which financially supported the project or programmed.

Tables and Illustrations

All the captions should be in the original language as well as in English, together with the texts in illustrations if possible. Tables are typed in the same style as the text and are denoted by numerals at the top. Photographs and drawings, placed appropriately in the text, should be clear, precise and suitable for reproduction. Drawings should be created in Word or Corel.

Citation in the Text

Citation in the text must be uniform. When citing references in the text, use the reference number set in square brackets from the Reference list at the end of the article.

Footnotes

Footnotes are given at the bottom of the page with the text they refer to. They can contain less relevant details, additional explanations or used sources (e.g. scientific material, manuals). They cannot replace the cited literature.

The article should be accompanied with a cover letter with the information about the author(s): surname, middle initial, first name, and citizen personal number, rank, title, e-mail address, and affiliation address, home address including municipality, phone number in the office and at home (or a mobile phone number). The cover letter should state the type of the article and tell which illustrations are original and which are not.